



**FACULTY OF TECHNOLOGY**  
**LUT ENERGY**  
**ELECTRICAL ENGINEERING**

**Master's Thesis**

**Application of Carbon Nanotubes in Rotating Electrical Machines**

Examiners: Professor Juha Pyrhönen  
M.Sc. Juho Montonen

Author: Victor Mukherjee

## **ABSTRACT**

Lappeenranta University of Technology  
Faculty of Technology  
Degree Programme in Electrical Engineering

Victor Mukherjee

**Application of carbon nanotubes in rotating electrical machine**

2014

Master's Thesis

83 pages, 19 pictures, 16 tables

Examiners: Professor Juha Pyrhönen

M.Sc. Juho Montonen

Keywords: Carbon nanotubes, chirality, electrical conductivity, mechanical strength, permanent magnet synchronous motor, permanent magnet synchronous generator, optimization, efficiency.

Demand for increased energy efficiency has put an immense need for novel energy efficient systems. Electrical machines are considered as a much matured technology. Further improvement in this technology needs of finding new material to incorporate in electrical machines. Progress of carbon nanotubes research over the latest decade can open a new horizon in this aspect. Commonly known as 'magic material', carbon nanotubes (CNTs) have promising material properties that can change considerably the course of electrical machine design. It is believed that winding material based on carbon nanotubes create the biggest hope for a giant leap of modern technology and energy efficient systems.

Though carbon nanotubes (CNTs) have shown amazing properties theoretically and practically during the latest 20 years, to the best knowledge of the author, no research has been carried out to find the future possibilities of utilizing carbon nanotubes as conductors in rotating electrical machines. In this thesis, the possibilities of utilizing carbon nanotubes in electrical machines have been studied. The design changes of electrical machine upon using carbon nanotubes instead of copper have been discussed vividly. A roadmap for this carbon nanotube winding machine has been discussed from synthesis, manufacturing and operational points of view.

## **ACKNOWLEDGEMENTS**

This work was carried out at the Department of Electrical Engineering, LUT Energy at Lappeenranta University of technology between 2013 and 2014. The research work was funded by LUT Foundation.

I would like to thank and pass my gratitude to my supervisor Professor Juha Pyrhönen for giving me the opportunity to work on such an interesting thesis topic, for his valuable guidance and wise suggestions during the thesis work. I would like to thank my second supervisor M.Sc. Juho Montonen for his priceless suggestions and support during the thesis work. Also I would like to pass my gratitude to Associate Professor Pia Lindh for her guidance during the thesis work.

I would like to thank to all my friends from India, Finland, Russia, Poland, Pakistan, Sri Lanka, Nepal, Iran, Mexico, Hungary, Nigeria and Rwanda for making my life so special and supporting me in different ways throughout my studies in Lappeenranta. I want to thank personally Arun Narayanan and Katerina Afanasyeva for their constant support and motivation during the thesis.

I want to express my sincere gratitude to my sister Ankita Mukherjee and her husband Suman Chatterjee for their constant motivation and inspiration.

Finally, I want to thank the most important people in my life, my father Bhaskar dev Mukherjee and my mother Jaita Mukherjee for their love and constant support through thick and thin of my life.

Victor Mukherjee

August 2014

Lappeenranta, Finland

## TABLE OF CONTENT

NOMENCLATURE .....	1
1. INTRODUCTION .....	5
1.1 MOTIVATION .....	5
1.2 CARBON NANOTUBES – STRUCTURAL CONCEPTS .....	6
1.2.1 NOMENCLATURE.....	6
1.2.2 CLASSIFICATION OF CARBON NANTUBES .....	6
1.2.3 CHIRALITY OF CARBON NANOTUBES .....	7
1.3 CARBON NANOTUBE PROPERTIES .....	11
1.4 CARBON NANOTUBE WIDE APPLICATIONS .....	15
1.5 RESEARCH OBJECTIVES AND ORGANISATION OF THE THESIS .....	16
2. MATERIAL DEVELOPMENT TREND .....	18
2.1 DIFFERENT PROCEDURES OF FORMING MACROSCOPIC NANOTUBES .....	18
2.2 MACROSCOPIC CNT CONDUCTOR TRENDS.....	20
2.3 BEST AVAILABLE SOLUTION FOR MACROSCOPIC NANOWIRE .....	21
3. PROVISIONAL PROPERTIES OF MACROSCOPIC WINDING.....	24
3.1 CNT AND COPPER COMPARISON IN EXTREME CONDITIONS .....	24
3.2 CNT COMPOSITE – DISCUSSION ON FEW SAMPLES .....	26
3.2.1 ELECTROMIGRATION.....	26
3.2.2 CNT DISPERSION.....	28
3.2.3 CNT AS INTERCONNECTS.....	28
3.3 ELECTROTHERMAL EFFECTS IN CNT.....	30
3.4 SEVERAL MACROSCOPIC RESULTS (MECHANICAL PROPERTIES).....	30
3.5 CNT ELECTRICAL CONDUCTIVITY–MACROSCOPIC BEHAVIOR.....	32
3.6 BENEFITS OF USING CARBON NANOTUBES IN ELECTRICAL MACHINES.....	39
4. MACHINE DESIGN ANALYSIS.....	42
4.1 BASIC DESIGN PROCEDURES .....	42
4.1.1 ROTOR DIMENSIONING.....	43
4.1.2 ELECTROMAGNETIC DESIGN OF STATOR AND ROTOR .....	44
4.1.3 ANALYTICAL PERFORMANCE ESTIMATION .....	50
4.2 CARBON NANOTUBE WINDING PMSM, 10 kW .....	50

4.3 CARBON NANOTUBE WINDING PMSM, 25 kW .....	55
4.3 CARBON NANOTUBE WINDING PMSM, 150 kW .....	59
4.3 CARBON NANOTUBE WINDING PMSG, 1 MW .....	63
5. CONCLUSIONS.....	71
REFERENCES .....	74

## NOMENCLATURE

### ROMAN LETTERS

$A$	linear current density	A/m
$a$	number of parallel branches	-
$a$	atomic lattice constant	m
$B$	flux density	Vs/m <sup>2</sup>
$b$	width	m
$D$	diameter	m
$e$	electromotive force	V
$f$	frequency	Hz
$H$	magnetic field strength	A/m
$J$	current density	A/m <sup>2</sup>
$h$	height	m
$k$	coefficient	-
$k_C$	Carter coefficient	-
$k_{w1}$	winding factor for the fundamental harmonic	-
$l$	length	m
$m$	mass	kg
$m$	number of phases	-
$N_{ph}$	number of turns	-
$n$	rotational speed	min <sup>-1</sup>
$P$	power	W
$p$	number of pole pairs	-
$Q$	slot number	-
$q$	number of slots per pole and phase	-
$R$	resistance	Ω
$r$	radius	m

$S$	area	$\text{m}^2$
$T$	torque	$\text{Nm}$
$t$	temperature	$^{\circ}\text{C}$
$t$	time	s
$U$	voltage	V
$z_Q$	number of conductors in a slot	-

### GREEK ALPHABET

$\alpha$	coefficient	-
$\delta$	air-gap	m
$\delta$	load angle	$^{\circ}$
$\eta$	efficiency	%
$\mu$	permeability	$\text{H/m}$
$\rho$	electrical resistivity	$\Omega\cdot\text{m}$
$\sigma$	electrical conductivity	$\text{S/m}$
$\tau$	pitch	m
$\Phi$	magnetic flux	Vs
$\varphi$	phase angle	$^{\circ}$
$\Psi$	flux linkage	Vs
$\omega$	angular velocity	$\text{rad/s}$
$\Omega$	mechanical angular velocity	$\text{rad/s}$
$\chi$	ratio of equivalent core length and air-gap diameter	-

### SUPERSCRIPTS

'	equivalent
'	transient

**SUBSCRIPTS**

0	initial value
c	Carter factor
e	electromagnetic
eff	effective
Fe	iron
Cu	copper
Mec	mechanical
Rad	radial
ex	external
m	magnetizing, airgap
max	maximum value
n	nominal value
p	pole
s	stator phase
t	tooth

**ABBREVIATIONS**

1D	one dimensional
2D	two dimensional
PMSG	permanent magnet synchronous generators
PMSM	permanent magnet synchronous motor
CNT	carbon nanotubes
SWCNT	single wall carbon nanotubes
DWCNT	double wall nanotubes
MWCNT	multiwall carbon nanotubes
CVD	chemical vapour deposition
UV/Vis-NIR	ultraviolet-visible near infrared
CTAB	cetyltrimethylammoniumbromide

CTAC	cetyltrimethylammonium chloride
OTAB	octadecyltrimethylammonium bromide
XTT	2,3-bis-(2-methoxy-4-nitro-5-sulfohenyl)-2H-tetrazolium-5-carboxanilide
LDH	layered double hydroxide
MTT	3-(4,5-Dimethylthiazol-2-yl)-2,5-Diphenyltetrazolium Bromide
DMF	dimethylformamide
NRAM	nonvolatile random access memory
DNA	deoxyribonucleic acid
MOSFET	metal-oxide-semiconductor field-effect transistor
IC	integrated circuit
MgB <sub>2</sub>	magnesium diboride
PAN	polyacrylonitrile
SiC	silicon carbide
CTE	coefficient of thermal expansion
CF	carbon fibre
PEEK	polyether ether ketone
PVA	poly vinyl alcohol
H <sub>2</sub> O <sub>2</sub>	hydrogen per oxide
SOCl <sub>2</sub>	thionyl chloride
PANI	polyaniline
SEBS	saturated styrenic elastomers
sPS	spark plasma sintering
PDDA	poly(diallyldimethylammonium chloride)
DOC	2,5-Dimethoxy-4-chloroamphetamine
NH <sub>4</sub> OH	ammonium hydroxide
Au	gold
Ag	silver

# **1. INTRODUCTION**

## **1.1 MOTIVATION**

The motivation of this thesis has emerged from the quest for the next generation technology which will considerably change electrical engineering. In 1991 Mr. Sumio Iijima of NEC discovered the so called “magic material” carbon nanotube with the hope of a new scientific horizon. Though, back to history, in 1952, (M.Monthioux, 2006) L.V.Raushkevich and V.M.Lukyanovich had shown the world some clear images of carbon nanotubes of 50 nm diameter in the Soviet Journal of Physical Chemistry, but the discovery was globally unnoticed as the article was written only in Russian.

Since 1991, carbon nanotubes have always been the centre of attraction in the genius minds around the globe. For the latest twenty three years since its discovery, the world has witnessed so many changes in different horizon of science, say in the field of electrical machines, vehicle technology, medical sciences, transistors, and computers and so on. It is a great interest in mind of the scientist of incorporating carbon nanotube (CNT) in the existing technology which we enjoy in our daily life, as it is believed that CNTs will bring a major change with our interaction with the technology. There are already profound researches in the field of transistors and micro electromechanical systems, where scientists are trying to incorporate carbon nanotubes to replace silicon. Very recently, scientists in Stanford University have manufactured a computer made entirely of carbon nanotube transistors which has shown amazing performance surpassing the power of regular computers (M.M.Shulaker, 2013).

Though considerable researches are going on different micro level, a noble pursuit for introducing carbon nanotube in macroscopic application has not been carried out before. The biggest motivation for this thesis is the quest to identify the application of carbon nanotubes in macroscopic application and more specifically in the field of electrical engineering. It is believed that electrical machines are at a very mature level of knowledge, so significant changes can only happen with the change of materials.

Carbon nanotubes, which have already proven to have superior capabilities, could revolutionize the whole design and even thinking among electrical engineering. In the following pages, a brief introduction in carbon nanotubes and their structural concepts will be provided to clarify a better understanding about the idea of the thesis.

## **1.2 CARBON NANOTUBES – STRUCTURAL CONCEPTS**

### **1.2.1 NOMENCLATURE**

Carbon nanotube, by its name is understandably made of carbon. By the word “nano” (meter) we mean a size of  $10^{-9}$  m. Carbon nanotubes comprise carbon compounds in very small size. But the reason for what makes it so special can be understood through the structural analysis of this material. Carbon has different allotropes which have different properties, e.g. diamond and graphite are both carbon. In a very similar way, CNT is an allotrope of carbon which is formed as a cylindrical nanostructure of carbon atoms. CNT is also known as bucky tube (Science Daily, 2013).

### **1.2.2 CLASSIFICATION OF CARBON NANTUBES**

Carbon nanotube can be considered as a single layer of carbon atoms which form a cylindrical shape. Basically it comes under the structural group of fullerene (M. S. Dresselhaus, 1996). One layer of carbon atom sheet in fullerene structural group is known as graphene, and when this graphene is rolled to form a cylinder, it is known as nanotube. Carbon nanotubes can be broadly classified into three categories depending on their structural differences which are governed by the number of graphene sheet rolls which means how many layer of carbon atoms are rolled. If only one layer of carbon atom is rolled to form a cylindrical structure, it is known as Single Wall Carbon Nano Tube (SWCNT), if two layers of carbon atoms are rolled to form a cylindrical structure, it is known as Double Wall Carbon Nano Tube (DWCNT). If more than two layers of carbon atoms are rolled to form a cylindrical structure, it is

known as Multi Wall Carbon Nano Tube (MWCNT) (M.Arnold, 2008). The different nanotubes are presented in Fig 1.1.

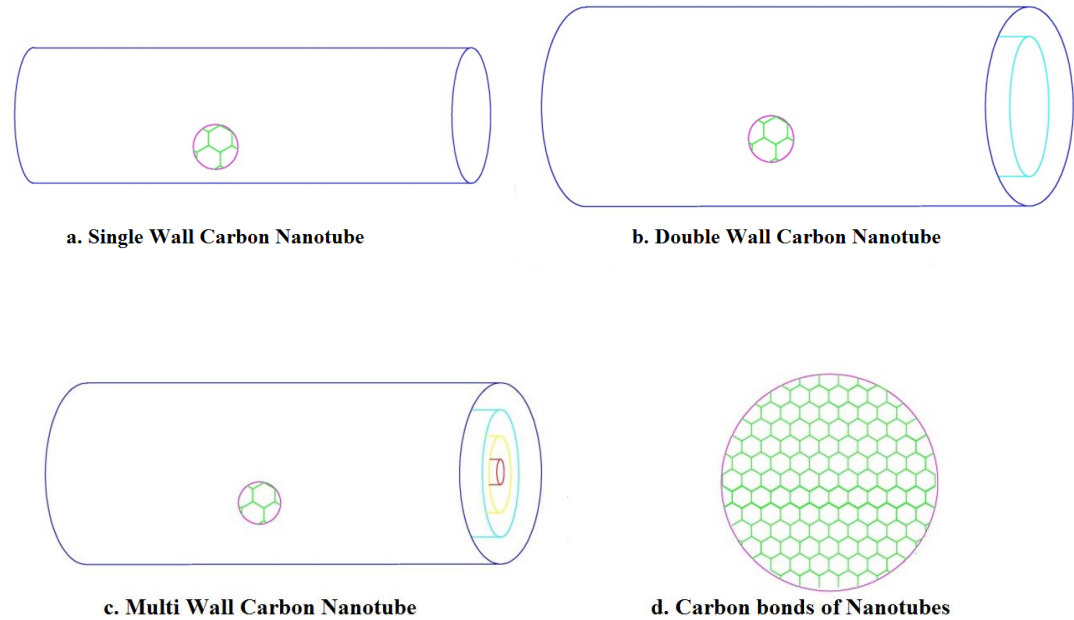


**Fig 1.1:** a) Single Wall Carbon Nanotube, b) Double Wall Carbon Nanotube, c) Multi Wall Carbon Nanotube d) Carbon bonds in Nanotubes

### 1.2.3 CHIRALITY OF CARBON NANOTUBES

Chirality is one of the important factors in the Carbon Nanotube technology. Controlled chirality is one of the major goals for CNT production. Lots of effort has been put to synthesis approaches, such as density gradient centrifugation (S.Ghosh, 2010). It is stated earlier that carbon nanotube is formed in principle like rolling a single layer of graphene. The rolling direction and rolling radius have a big impact on the CNT properties. There are two main aspects about the rolling. Radius is tried to be kept constant. Where the main variation arises is the angle in which it is rotated to form the tube. The angle of rotation is known as chirality, Fig 1.2. Rolling up of graphene is governed by a chiral vector to form a cylinder. The circumference of CNT is calculated by its chiral vector  $C_h$  which is defined as

$$\mathbf{C}_h = n\mathbf{a}_1 + m\mathbf{a}_2 \quad (1.1)$$

Here  $n, m$  are integers known as the chiral indices and  $\mathbf{a}_1, \mathbf{a}_2$  are the unit vectors of the graphene lattice. (B.Liu, 2012)

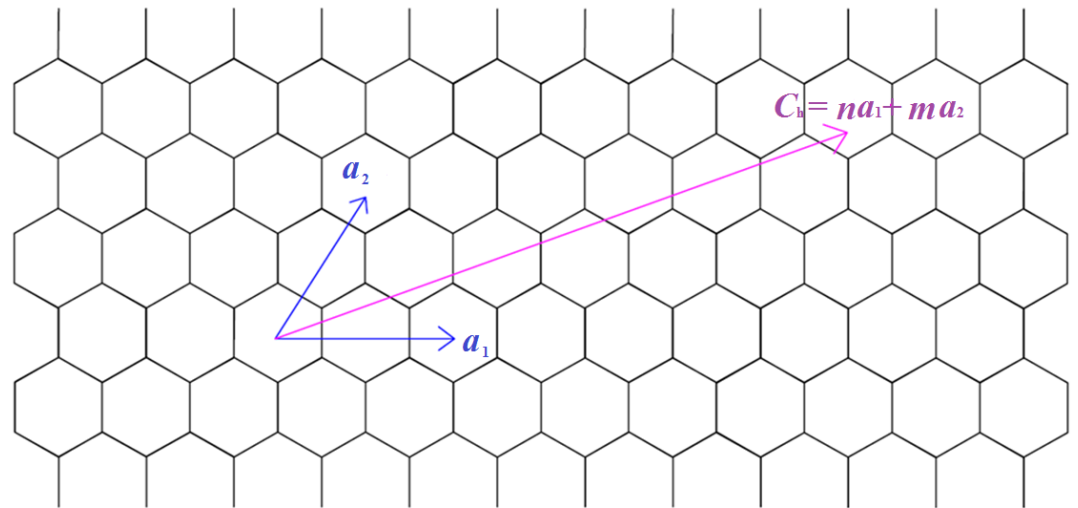


**Fig 1.2:** Chirality in the lattice. Rolling is performed in the direction of the chirality vector  $\mathbf{C}_h$ . (B.Liu, 2012)

In Fig (1.2), it is clearly understood that the variation of  $n, m$  change the orientation of CNT rolling. This is a vital concept, because the properties of CNT are highly dependent on the orientation. There exist two extreme cases – when  $n = m$  or  $m = 0$ , Fig 1.3 (B.Liu, 2012) .

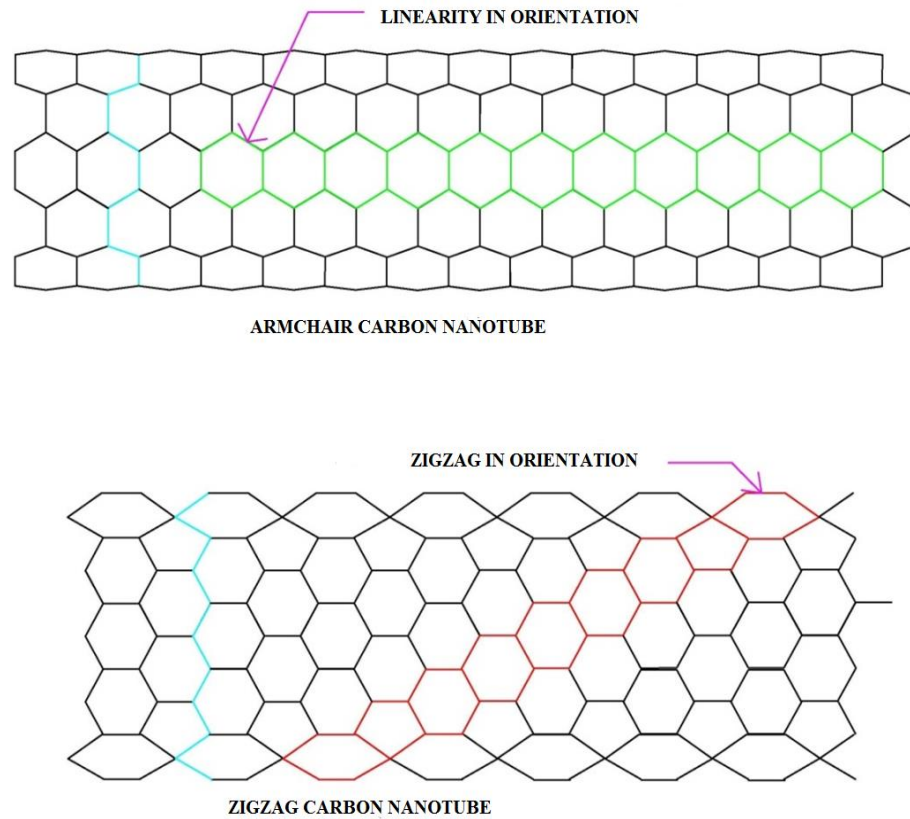


**Fig 1.3:** Orientation of Armchair nanotube ( $n = m$ ) and Zigzag nanotube ( $m = 0$ ) (B.Liu, 2012)

So in the first case where  $n = m$ , the nanotubes are known as Armchair Carbon Nanotubes. It is worth mentioning that the armchair carbon nanotubes are the carbon nanotubes which show the best properties because of their orientation. It is very difficult to synthesize and costly as well.

The next extreme case is when there is no vertical index of chirality vector i.e. when  $m = 0$ . In this case the nanotubes will be oriented in complete haphazard manner (F.Silly, 2005). They are known as Zigzag Carbon nanotubes. They have the worst properties among all the carbon nanotubes. All the other chirality possibilities lie between the value of  $m$ , i.e.  $0 < m < n$ . There is an equation to calculate the diameter  $D$  of the CNT based on the value of  $m$  and  $n$  which is given by

$$D = \frac{a}{\pi} \sqrt{n^2 + nm + m^2} = 78.3 \sqrt{(n^2 + nm + m^2)} \text{ pm} \quad (1.2)$$

In Equation (1.2), the atomic lattice constant  $a = 0.246 \text{ nm}$  (D.Resaco, 2014).

The behaviour of carbon nanotube to be metallic or semi-conductive is also dependent on the difference  $(n - m)$ . Actually the rolling action alters the symmetry of the planar system and imposes a specific direction with respect to the axial direction of hexagonal lattice. Depending upon the relation between axial direction and the unit vectors describing the lattice, the properties of CNT show its variance. If  $(n - m) = 3 \cdot j$ , where  $j = 0, 1, 2, 3$  etc, the carbon nanotubes will be metallic in nature. CNT with  $(n - m) = 3 \cdot j + 1$  or  $(n - m) = 3 \cdot j + 2$  will be semiconductors with a band gap which varies inversely with the diameter.

In this thesis our primary focus will be on metallic CNTs, but a brief concept of the utility of semi-conductive CNT will also be provided. A great way to control the chirality is the usage of liquid crystal being doped with a small quantity of CNT having a net chirality, and the mixture is found to exhibit an average mechanical twist over macroscopic dimension (R.Basu, 2011). Liquid crystals have good capabilities to transfer their long range orientation order into dispersed nano-materials like CNT, Quantum Dots, nano-rod and various shaped colloids (G.Iannacchione, 2008). It is worth mentioning that low concentration of CNT may be organized in a nematic medium over macroscopic dimension, providing a fascinating system that involves an anisotropic colloidal dispersion in an anisotropic medium (M.D.Lynch, 2002). A dilute CNT suspension in a nematic liquid crystal is stable as dispersed CNTs. Without large agglomerates, it does not distort the director field significantly (R.Basu, 2011). As a result, the suspended nanotubes share their intrinsic properties with the liquid crystal matrix like electrical conductivity and dielectric anisotropy (I.Dierking, 2005).

### 1.3 CARBON NANOTUBE PROPERTIES

In this paragraph a brief idea about the distinguished properties of CNT will be provided revealing the true justification of the possibility of “magic material”, though more application specific discussions will be done in the next chapter.

Pristine armchair carbon nanotubes are highly conductive in nature. As CNT is one dimensional in nature, the charge carriers can travel through nanotubes without scattering which is commonly referred as “Ballistic Transportation”. The absence of scattering helps carbon nanotube to carry very high current density, theoretically in the order of  $100 \text{ MA/cm}^2$  (B.Q.We, 2001). This helps creating less Joule heating and thereby opens a new possibility for carbon nanotube to operate as an electrical carrying conductor. These properties are for metallic CNTs. In semi-conductive CNTs, carrier mobilities have been observed in the range of  $10^5 \text{ cm}^2/\text{Vs}$  (B.M.Kim, 2004). SWCNTs have also shown its superconductive nature albeit with transition temperatures of 5 K (Z.K.Tang, 2001). CNTs are also thermally very conductive which make it quite suitable for phonons. Theoretically, it can reach a thermal conductivity of up to  $6000 \text{ W/(Km)}$  (J.W.Che, 2000) (M.A.Osman, 2001). Though this value has not been reached yet, but around  $200 \text{ W/Km}$  has been measured in laboratory (J.Hone, 2002). The conductive nature of CNTs can also be understood from their band gap demonstration, Fig 1.4. In Fig 1.4,  $V_1$  represents the energy state of the first valence band,  $V_2$  represent the energy state of second valence band,  $C_1$  represent the energy state of the first conduction band,  $C_2$  represent the energy state of the second conduction band. In case of metallic SWCNT,  $V_1 \rightarrow C_1$  corresponds to the first Van Hove optical transition which is represented by  $E_{11}$ , for semi-conductive SWCNT,  $V_2 \rightarrow C_2$  corresponds to the second Van Hove optical transition which is represented by  $E_{12}$  (D.Tomanek, 2014). Energy gap in density of state varied between 0.6 eV to 1.8 eV, where 0.6 eV fits in expected semiconducting band gap and 1.8 eV fits in expected metallic band gap (J.W.G.Wildoer, 1998).

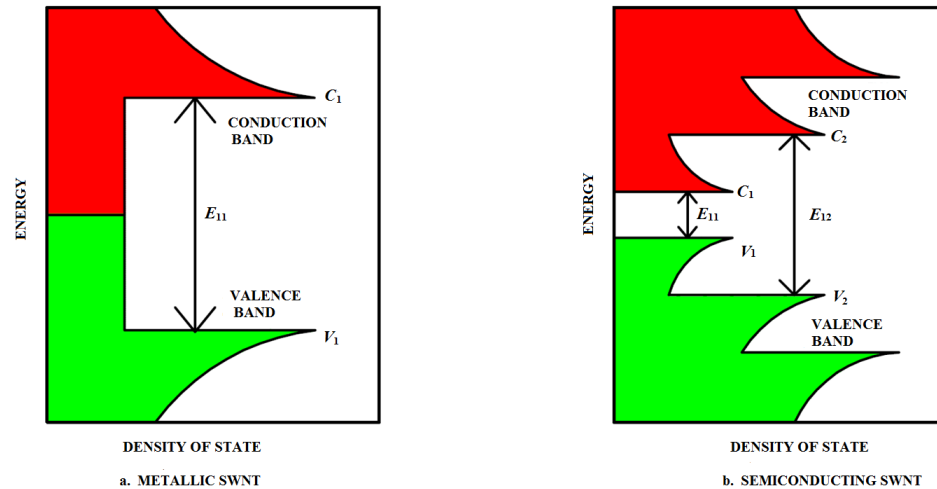


**Fig 1.4:** Band gap demonstration of Carbon Nanotube. (J.W.G.Wildoer, 1998)

In practice, scientists have so far not been able to create a method to just roll long SWCNTs from graphene and therefore pure SWCNT is not easily available. As CNTs are “one dimensional” structure (only length), they have great flexibility and high surface energy. CNTs try to aggregate with one another and form big bundles. These bundles can contain both metallic CNTs and semi-conductive CNTs in a complete random orientation and in huge numbers. Certainly such bundles’ properties are not as good as those of the pure CNT. It is also very difficult to segregate the pure CNTs like SWCNTs from the bundle and here lies the future research possibility of acquiring pristine nanotubes, which have a great possibility of the future technology. The segregation methods will be discussed in details later.

Mechanically CNT is very strong; it is hundred times as strong as steel with just the one sixth of its density (gizmag, 2013). The mechanical properties of CNT can vary based on different things, especially the way it is synthesized, whether the CNT fibres are SWCNT or MWCNT, whether they are armchair or zigzag etc. It also depends on the usage of composite materials with CNT if used and again the nature of that composite material. Chemical vapour deposition is one way of synthesizing CNT influences the strength of CNT fibres. Theoretically, it is expected that CNT will show superior mechanical properties. Its Young modulus is in the range of 1.06 TPa

(B.T.Kelly, 1981). The value is estimated over the calculation of the strength of C–C bonds. In 1993, Dr. Overney has calculated the rigidity of short SWCNT using local density calculation to determine the Keating potential of the material (G.Overney, 1993). The Young Modulus thus calculated was around 1500 GPa. It is assumed that CNT will have mechanical strength in the range of at least 1 TPa (J.P.Lu, 1997). Macroscopic application of CNT is highly dependent on its mechanical strength. In 1997, atomic force microscope was used by Prof Wong and his team, and they have successfully calculated a Young Modulus of 1.28 TPa (E.W.Wong, 1997). In 2000, another stress strain analysis was carried out, and CNTs have shown Young Moduli between 0.27 – 0.95 TPa. The strains are up to 12 % which is quite a good result (M.Yu, 2000). But it is to be remembered that the strength of CNT lies in the axial direction. There are several cases where it is observed that CNT is soft in the radial direction. It has shown radial elasticity which means that even van der Waals force can deform two adjacent nanotubes. It can happen because, as with same outer diameter of MWCNT, the internal diameters of the CNTs can be different. In MWCNT, the inner nanotube core may slide with almost zero friction over the outer tube which makes it ideal for nano–size rotational bearing. The precision for its one dimensional structure can help to design a motor with very small size (S.Jayronia, 2013). Though the optical properties are not very clear for carbon nanotubes, it is expected that CNT can open a new possibility in that field, too. High optical transmittance and low sheet resistance is a very exclusive property which CNT can offer.

The health effects of CNTs form a very important issue in modern CNT research. There are different opinions and facts about the health effects. What we can subtly assert is that the adverse effects of CNTs depend upon the nature of CNTs, the way it is synthesized and most importantly the way it is spun in the macro level. It also depends on the internal structures, the surface area and the surface chemistry. If CNTs are inhaled, they can be easily absorbed by human body and can cause problems in lungs. In some advanced studies, it has been observed that when rats are exposed to carbon nanotubes, rats started facing pulmonary injuries in multifocal granulomas. In

some other experiment, it has been found that exposure of human keratinocyte cells to carbon nanotubes showed increased oxidative stress and accumulation of peroxidative products, followed by antioxidant depletion. Biochemically, there are loss of cell viability and morphological changes. Also, it has been observed that CNT can causes skin irritation and allergy risks. (S.K.Manna, 2005)

Though lot of experiments and observations on human health has to be done, but it is believed medically by many scientists that the unique properties of carbon nanotubes may lead to unique health hazards. Fig 1.5 shows some results of health problem studies.

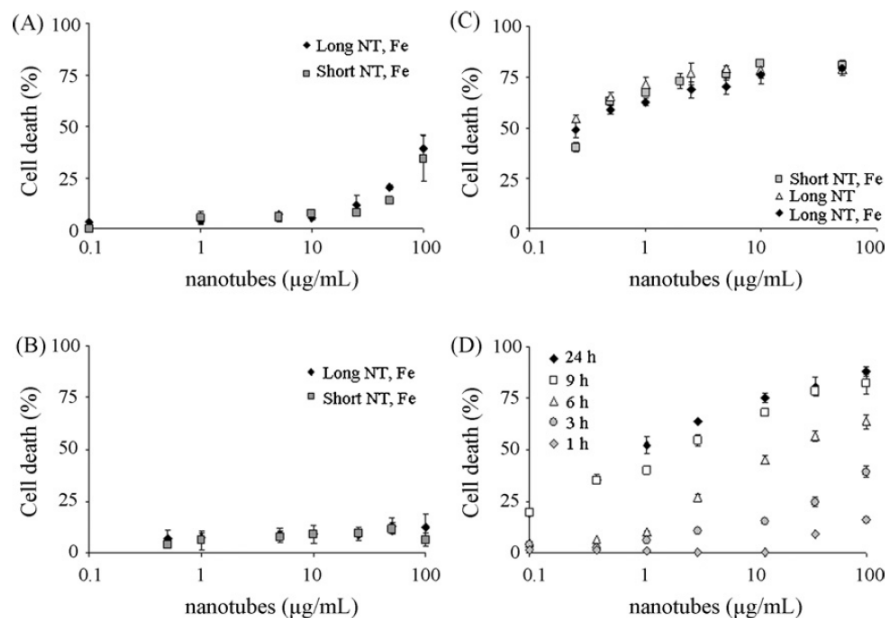


**Fig 1.5:** Cell death induced by MWCNT. A549 cells were exposed during 48 h to increasing MWCNT concentrations. Cell death was assessed with LDH (A), XTT (B) or MTT (C) and expressed as a percentage of the control (untreated cells). The kinetics of MTT response was evaluated when A549 cells were exposed to long MWCNT with Fe (D). (A.S.Deckers, 2008). Original figure from the publication has been used with copyright permission.

## **1.4 CARBON NANOTUBE WIDE APPLICATIONS**

Due to their unique properties CNTs can have exclusive applications in a wide range of fields. Mechanically when used as a composite material, it can show very good strength which can be used in vehicles, ships or aircraft parts. It will be light weight and strong which can open a door in the automotive sector. The polymer fibres when synthesized with CNTs can be used to make light weight strong ropes, which can be widely used in cranes and in different earth moving equipment. CNTs can also be used to form electrostatic painting which can be used in car body panels and mirror housing. Due to its non-adhesiveness towards water, it does not allow water to stay on its surface which makes it ideal for coating. There are instances of carbon nanotubes used as a coating on the blades of wind turbine. It is a possible solution for cold countries like Finland where snow can cover up the turbine blade in winter (R.H. Baughman, 2007). CNTs are used widely now a day in sports equipment. For instance it is widely used in tennis bats and ice hockey bats manufacturing. (Hockeyworld, 2014)

It has also good thermal conductivity which makes it ideal to use it in electronic components and elastomers. CNTs are widely used in manufacturing transistors and MOSFETs as they have shown very good property in interconnection. CNT made computers have already opened a new door of technology for next generation. Due to its high current density capability and anti-static behaviour, it can be used very successfully in fuel filler caps, automotive fuel lines, fuel filter housing, fuel hoses, IC trays, carrier tapes and intermediate containers. Electrical wire for transmission and power distribution can be completely reshaped with the incorporation of the CNTs. (Abate, 2013)

Electrical machines, can in principle, be made very efficient using carbon nanotube windings instead of copper windings. In principle it will decrease the machine loss considerably. Carbon nanotubes can be synthesized with different composites which can be widely used in super capacitors. CNT-made super capacitors are growing very

popular presently as they have higher energy storage capacitance than normal super capacitors and have the potential to be used instead of batteries. (K.Gong, 2009)

Apart from the above, CNT made artificial bio-fibre can be used in organ replacement therapy (B.S.Paratala, 2011). CNT fibres can be used in textile industry; they will be dust proof. Due to its structural benefits, it can be used in manufacturing paper battery, carbon nanotube actuators and hydrogen storage. SWCNT has strong UV/Vis-NIR absorption characteristics, which makes it quite ideal for using in solar panels. Application of CNT in other fields like radar absorption, optical power detectors, mechanical memory system (NRAM), nanoradio, DNA detection are carried on by different scientists across the globe. The ultimate dream of space elevator can only be successful in the future by the superior and pragmatic applications of carbon nanotubes. (R.H. Baughman, 2007)

## **1.5 RESEARCH OBJECTIVES AND ORGANISATION OF THE THESIS**

Carbon nanotubes have potential to start a revolution in the field of electrical machines. But unfortunately, macroscopic nanotubes are for the moment very difficult to manufacture. This thesis will try to relate carbon nanotube applications in the field of rotating machines. Briefly the research objective has four major aspects which are organized in four different chapters described below.

- 1. Material Development Trend:** Literature analysis about the improvement of carbon nanotube components from the point of incorporation in electrical machines will be demonstrated. It is worth mentioning that though carbon nanotubes show great properties in nano level, so far they have not been capable of holding the same type of properties in macroscopic level. Several modern researches are going on for stable macroscopic nanotube synthesis. Based on that, the best solution for the rotating machine is proposed.

2. **Provisional Properties of macroscopic winding:** Though the carbon nanotube is in the very early stage for using in the electrical machine a brief study will be done on the provisional properties. It is worth mentioning that with the usage of different spinning techniques, composites materials the macroscopic properties for carbon nanotubes will change in the future. Several results for the properties of CNTs in macroscopic level are documented with the trend of improvements over years.
3. **Machine Design Influence:** A brief study has been done about the electrical machine design changes considering hypothetical carbon nanowire with 2 times the conductivity of copper in the machine operating temperature. Comparison model for existing permanent magnet synchronous machine will be done with such hypothetical carbon nanotube conductors wound machine.
4. **Conclusion:** Conclusions for the thesis, obstacles of using CNTs in rotating electrical machines and future work on this subject have been discussed.

## **2. MATERIAL DEVELOPMENT TREND**

CNTs have 100 times the strength of steel but only one sixth of its density. It also theoretically has better electrical conductivity than copper. Therefore, carbon nanotubes have been a promising research field since their discovery (gizmag, 2013). The problem is to convert that kind of behaviour from the nano level to macroscopic level and retain the good properties. Recent breakthrough in the macroscopic model of CNTs has bought us the hope of using them as electrical wires with multiple utilities. The macroscopic nature of CNT depends on different synthesis process and composition factors. In the following paragraphs, each of those factors will be discussed which influence the resistance and nano-wire tensile strength. The material development ways will be analysed which will help us to select future current carrying materials to be utilized in rotating electrical machines.

### **2.1 DIFFERENT PROCEDURES OF FORMING MACROSCOPIC NANOTUBES**

Macroscopic CNT fibres have the properties to form higher strength, lighter weight, thermally and electrically conducting structural elements at lower cost than other forms of SWCNT (W. Zhou, 2004). The electrical properties may be, in principle, utilized in highly efficient transmission of electricity or even making more efficient electrical machines than with copper.

In direct fibre synthesis from SWCNT, length up to 20  $\mu\text{m}$  has been achieved by using 1,3 dicyclohexylcarbodiimide to polymerize oxidized SWCNT into strands with 50–150 nm in diameter (X.H. Li, 2003). Graphitization of the ribbons for two hours under 2200°C under argon with pressure of 0.5 MPa resulted in an increase ribbon density from 1.1 to 1.5  $\text{g}/\text{cm}^3$ . Aligned CVD (Carbon Vapour Deposition) grown nanotubes have assembled into yarns up to 30 cm length by arranging them in arrays of several

hundred micrometers in height in a process similar to drawing silk out of cocoon (K. L. Jiang, 2002).

In electrophoretic spinning, fibres are electrophoretically spun from purified laser vaporization grown SWCNTs dispersed in *n,n* dimethylformamide (DMF) at concentrations of about 0.01 mg/ml (H.H.Gommans, 2000). But this is not very common. SWCNT fibres are mostly produced by the solution spinning process. Solution spinning is normally more complex than melt spinning as the solidification of fibres requires additional steps. The fibre forming material needs to be dissolved or finely dispersed into a solvent. Then the solvent has to be extracted after the extrusion to form the solid fibre. So, solution spinning is normally preferred to produce fibres from materials that decompose before reaching their melting point or do not have a proper viscosity for stable fibre formation (V.A.Davis, 2004). Solution spinning is widely classified into two main groups: dry solution spinning and wet solution spinning. For both types, the spinning solution consists of the polymer dissolved in the solvent. The solution is extruded through one or multiple orifices from the spinneret, the solvent is taken out solidifying the fibre. Dry spinning is applied for systems like cellulose acetate in acetone where the solvent is quite volatile, that means it can be easily vaporised from the fibre during its formation. Wet spinning is preferred when the polymer is dissolved in a non-volatile solvent which needs to be extracted by using another liquid which is miscible with the solvent but can not dissolve the fibre forming material. In wet solution spinning, the solution passes through an air gap, and then enter into a coagulation bath. It is also known as dry jet wet spinning. The air gap helps for better elongation and cooling of the spinning solution before coagulation (V.A.Davis, 2004). We have to remember that the phase behaviour and related rheological properties of the dispersion highly influence the selection of spinning solution concentration, coagulation and spinning process variables and the alignment in spun fibres. The final fibre properties are depended on these variables as well as subsequent washing, drawing, drying and annealing process (G.D.Kiss, 2003). It has been observed that by varying the composition of iodine doped multi walled nanotubes from 0.2 to 4 wt-%, electrical conductivity increases significantly up to

$67.68 \cdot 10^4$  S/m (M.S.P.Sarah, 2012). Polyacrylonitrile (PAN) can be used as carbon precursor which have significant applications in energy storage (T.V.Sreekumar, 2004). It has been observed PAN/SWCNT fibres produced by dry jet wet solution spinning have a very high tensile strength than pure PAN, i.e. tensile modulus has been doubled from 7.9 GPa to 14.2 GPa. SWCNT/acid dispersion for producing neat fibres may be the best option for applications with the most demanding thermal and electrical requirements (V.A.Davis, 2004). Another good way of producing macroscopic MWCNT is dispersing CNT (2g) in water solution (100 ml) under sonication (40 W, 30 min) (Y.Liu, 2012). The development of spinning technologies with the improvements in SWCNT production, purification and functionalization will result in the production of the best nanowire through which we can model a superior electrical machine.

## **2.2 MACROSCOPIC CNT CONDUCTOR TRENDS**

If we consider the cross-sectional area of the CNT walls, the elastic modulus can be even 1 TPa and tensile strength of 100 GPa was measured for individual MWCNT (B.Peng, 2008). The strength is 10 times that of an industrial fibre and can carry current up to  $10^9$  A·cm<sup>-2</sup> (B.Q.We, 2001). The CNT walls on individual basis can possess metallic or semi-conductive property depending upon the orientation of the graphene lattice with respect to the chirality. Individual SWCNTs have thermal conductivity of  $3500 \text{ W m}^{-1}\text{K}^{-1}$  based on the wall area which is even higher than in diamond (E. Pop, 2006). But these properties are very difficult to achieve. The latest nano-wire in macroscopic form has been discussed earlier. It has very good properties but not as outstanding as individual SWCNTs in nano form. We have to develop more knowledge on CNT chirality, diameter length and purity related to catalyst composition and process conditions. May be in the future, with more superior formation of SWCNT/MWCNT nano-composites, we will be able to cross the barrier of discrepancy in macroscopic form. CVD can be very important in the future for

producing high volumes of CNT, using fluidized bed reactors enabling uniform gas diffusion and heat transfer to metal catalyst nano particle (M.Endo, 2006). We have to remember that large scale CVD methods can yield contaminants that can influence CNT properties, which necessitate costly thermal annealing or chemical treatment for waste removal (Q. Zhang, 2011). Even it can affect the CNT side walls and shorten CNT length. SWCNT synthesis by CVD needs more acute process control than MWCNT synthesis and therefore bulk SWCNT is more expensive than MWCNT. Another alternate way is to include self-aligned growth of horizontal and vertical CNTs on substrates coated with catalyst particles and production of CNT sheets (K.Koziol, 2007). CNT resins are used to increase the fibre composites (J.N.Coleman, 2006). Special application can be seen in the manufacturing of strong, lightweight wind turbine blades by using carbon fibre composites with CNT enhanced resins. CNT-SiC fabric impregnated with epoxy, CNT alumina fabrics have shown improved toughness (E. J. Garcia, 2008), and applications like lightning strike protection, de-icing and structural health monitoring for air craft (V.P.Veedu, 2006). Also high performance fibres of aligned SWCNT can be prepared coagulation based spinning of CNT suspension which is attractive for decreasing the price of SWCNT production. Thousands of spinnerets can operate in parallel and CNT orientation can be achieved by liquid crystal formation. (N.Behabtu, 2013)

### **2.3 BEST AVAILABLE SOLUTION FOR MACROSCOPIC NANOWIRE**

The light weight CNT fibre formed in Rice university and Teijinaramid has achieved high specific strength of polymeric and carbon fibres, along with achieving the high specific electrical conductivity of metals and the specific thermal conductivity of graphite fibres (N.Behabtu, 2013). Two distinct routes have been developed for manufacturing the CNT fibres. One way is to employ a solid state process wherein CNT are directly spun into a fibre from the synthesis reaction zone (K.Koziol, 2007). The alternate fibre production is done by wet spinning where premade CNT fibres are dissolved or dispersed in fluid, and extruded out of a spinneret and coagulated into a

solid fibre by extracting the dispersant (B.Vigolo, 2007). In Rice University, “*high quality CNTs were dissolved in chlorosulfonic acid at a concentration of 2 – 6 weight percent (wt-%) and filtered to remove particles, in order to form a spinnable liquid crystal dope. The dope was extruded through a spinneret (65 to 130 $\mu$ m diameter) into a coagulant (acetone or water) to remove the acid. The forming filament was collected onto a winding drum. The linear velocity of the drum was higher than the dope speed at the spinneret exit, to ensure high CNT alignment by continuous stretching and tensioning of the filament. The fibres were further washed in water and dried in oven at 115°C.*” (N.Behabtu, 2013)

Fig. 2.1 illustrates CNT wire wound around a core.



**Fig 2.1:** Carbon fibre produced by Teijinaramid and Rice University which has shown excellent property. Photo by Marcin Otto, Teijinaramid

The fibres have good mechanical, electrical and thermal properties. Tensile strength, elongation to break is measured from tensile break test on macroscopic filaments cut from a large spool. The average tensile strength is  $1.0\pm 0.2$  GPa and the average modulus of elasticity is  $120\pm 50$  GPa. The average elongation for breaking for these fibres is  $1.4\pm 0.5\%$ . Being measured by two and four point probe methods on 25 mm single filaments, on average  $2.9\pm 0.3$  MS/m (resistivity of  $35\pm 3$   $\mu\Omega$ cm) at room temperature is displayed, but when doped with iodine, it shows even a better characteristic like  $5\pm 0.5$  MS/m (resistivity of  $22\pm 4$   $\mu\Omega$ cm). The average thermal

conductivity of  $(380 \pm 15)$  W/(Km) on 1.5 mm long sample has been found by using 3 omega method. Iodine doping doubled the thermal conductivity.

The nanowire mentioned above is the latest and most stable macroscopic nanotube with the best present day characteristics. The properties can be taken as a reference to model an electrical motor. The conductivity is, however, relatively low compared to that of copper, but the strength is significantly higher than copper. (N.Behabtu, 2013)

In this chapter we have seen the practical model of nano-wire through which we can conceptualize the future electrical machine. The different composite materials influence on the properties of CNTs has been discussed. The importance of doping, especially iodine doping which increases the electrical properties of nanotube have been discussed. Also, different macroscopic processing especially CVD and spinning technologies have been discussed to provide the understanding of the manufacturing of macroscopic nano-fibres. The different macroscopic utilities have been discussed in brief and few other techniques for processing that have been mentioned. In the following chapter, the macroscopic properties of CNT from the viewpoint of using in electrical machine and its benefits are discussed.

### **3. PROVISIONAL PROPERTIES OF MACROSCOPIC WINDING**

The provisional properties of CNT winding are of great interest. Till the date of writing this thesis, to the best knowledge of the writer, no research has been reported out about the provisional properties of CNT wire when used mainly in a rotating electrical machine winding. We know that due to CNT's single dimensionality and high current density factor, it can revolutionize the machine design if also the conductivity can be brought close to the theoretical values of CNT. But before the design process (which will be discussed in the following chapter), it is important to identify the provisional properties of nanotubes in the future based on the current available knowledge. In this chapter, a brief comparison will be done with copper and CNT. Also electrical properties like conductivity and mechanical properties like tensile strength and Young modulus of different CNT composites will be analysed. Due to the implementation of different spinning techniques and vapour deposition methods, which has been improved considerably over the latest years, the values of electrical and mechanical properties will vary considerably over years.

#### **3.1 CNT AND COPPER COMPARISON IN EXTREME CONDITIONS**

CNTs have the theoretical capability to overcome the limitation of classically employed conductors. The only hindrance is its manifestation in the macroscopic functional structures like wires and cables. A recent comparative study has shown that CNTs survive salty or highly acidic conditions. Also CNTs do not degrade over long time period in certain harsh conditions. CNTs have density one sixth of the density of copper and have the capability of conducting with three orders higher current densities than copper (S.Hong, 2007). For these reasons several modern researches are going for macroscopic synthesis keeping the superior properties intact. Though several processes have been investigated involving wet chemical like super acids (L. M.

Ericson, 2004), or other complicated matrices, or pre synthesizing CNTs array to draw from it (M.Zhang, 2004) or without twisting (X.B. Zhang, 2006 ). In a very modern approach, feedstock of carbon precursor like methane, ferrocene catalyst and thiopene promoter are introduced into a vertical reactor at 1200 °C in hydrogen atmosphere. CVD causing formation of an aerogel made up of CNTs, which are then drawn out from the reactor and transferred in a constant fashion onto a fast spinning winder (Y. Li, 2004). The winder is covered with transparent acetate sheets where the CNT aerogel are deposited as fibre. When the single fibres are cut into 10 cm with  $0.25\pm 0.004$  mm in diameter, it shows the resistance within  $503\pm 47$   $\Omega$ ; for a similar copper wire,  $2.0\pm 0.1$   $\Omega$  is observed. (D.Janas, 2013)

Copper wire show a lot of changes in resistivity, i.e. decrease in conductivity in harsh conditions. So, copper wire is not the best option for degrading conductivity in prolonged time, whereas surprisingly, CNT wire has shown very stable behaviour when it comes to extreme conditions. Rather the extreme condition has a positive influence, primarily because the moisture was shown to undergo n-type doping. But after a few days, the conductivity reaches equilibrium. (A.Zahab, 2000)

For acidic atmosphere also the conductivity surprisingly increases. The possible explanation is p-type dopant as acid treatment increases the delocalized holes (R.Graupner, 2003). In a lead acid battery, where the metal part often gets under corrosion, CNT wire can be really beneficial for replacing copper. Also, CNT wire will provide significant reduction in the insulation cost, flexible and lighter wires compared to the required thicker insulation needed by copper. It will eliminate the problem of broken electrical circuit as a consequence of crack in copper wire insulation, so the operation with CNT wire will be very smooth. (D.Janas, 2013)

## 3.2 CNT COMPOSITE – DISCUSSION ON FEW SAMPLES

Several researches are going on to understand how effectively CNT can be coupled with solders, epoxy composites and solder joints and the influence on reliability. The best potential of CNT in interconnected applications rely on the density of nanotubes in the area, their chirality, the interaction between copper and CNTs, a good wetting in the matrix, and orientation of the nanotubes in the matrix (Q.Chen, 2007).

### 3.2.1 ELECTROMIGRATION

A significant increase in the electro migration resistance of copper can be found without compromising its conductivity. CNT is hydrophobic in nature. CNTs do not form a uniform dispersion in water based solution due to strong van der Waals forces. So, surfactants are added to reduce the surface energy when dispersed in water solutions. Surfactants are normally two types: cationic and anionic. Cetyltrimethylammoniumbromide (CTAB), Cetyltrimethylammonium chloride (CTAC), Octadecyltrimethylammoniumbromide (OTAB) are the main cationic surfactants which introduce positive charge in nanotubes and help in the prevention of flocculation. Upon dispersion in a copper sulphate bath for electrochemical deposition, positively charged metal ions and the nanotubes are electrochemically reduced which help the overall reaction. Anionic surfactants like Nafion produce negative charge to the nanotubes, and hence they repel the positively charged metal ions. The coefficient of thermal expansion (CTE) of the composite is estimated between  $3-6 \cdot 10^{-6}/K$  within the temperature range of  $25^{\circ}C$  to  $120^{\circ}C$ , with 18 % proportion of SWCNT. The CTE value of the CNT Copper composite is one fourth of the CTE of pure copper ( $17 \cdot 10^{-6}/K$ ), which implies that CNTs can eradicate the problem of CTE mismatch in semiconductor. The thermal conductivity of the composite is approximately  $640 W/(Km)$ , 66 % more than in copper. **The electrical resistivity is decreased by 40 % for this CNT copper composite, leading to a**

**remarkable result of  $1.22 \cdot 10^{-6} \Omega\text{cm}$  compared with pure copper  $1.72 \cdot 10^{-6} \Omega\text{cm}$ .**

However, no macroscopic fibre has been produced with this CNT copper composite till the date of writing this thesis. (L.Aryasomayajula, 2013)

Though polymer composite of CNT does not possess as high conductivity as pure armchair SWCNT, it is worth mentioning that electrical and thermal conductivities of CNT/epoxy composites are better in properties to those equivalent specimens with T300 carbon fibres (CF) which are widely used in industry (J.J.Vilatela, 2012). The CNT fibres are produced by direct spinning of a CNT aerogel directly from the gas phase during CNT growth under chemical vapour deposition, thiophene, ferrocene and methane as precursors and hydrogen as carrier gas. The fibres are collected with a speed of 10–30 m/min and densified simultaneously by spraying a mist of acetone. (K.Koziol, 2007)

While adding CNT fibres, it results in a large increase in axial electrical conductivity, the highest value obtained is 3600 S/m for the CNT fibre and 560 S/m for the CF. The maximum thermal conductivities are 23 W/(Km) and 5.3 W/(Km) for 10 % and 30 % mass fraction of CNT fibre and CF respectively. CNT fibres have a very specific yarn like structures through which surface area quite much higher than traditional fibre can be accessed. Incorporating CNT fibres does not disrupt the CNT bundle network, the electrical conductivity of the composite is  $1.6 \cdot 10^4$  S/m per unit mass fraction of fibre. CNT fibres provide an effective increase in the thermal conductivity to the composite which is 157 W/(Km) per unit fibre mass fraction (J.J.Vilatela, 2012). CNT length and overlap is very important in optimizing the electrical and thermal conductivities. MWCNT yarns being spun from tall MWCNT arrays have good properties compared with high conductivity CNT fibres. Simulations have suggested that proper optimization of CNT overlaps and length along with improved quality of fibres can provide few MWCNT better conductivity coefficients than copper and other high performance carbon fibres (M.B.Jakubinek, 2012).

### 3.2.2 CNT DISPERSION

Nanotube dispersion is a very important factor in identifying these types of superior properties in macro scale. As CNTs have large aspect ratio that creates large van der Waals forces, it make the CNT to stick together to form strong bundles. One of the major challenges is the fabrication of CNT films separating them from the CNT tubes. CNT dispersion can be divided mainly into four categories which are – (1) surfactant as dispersion aids (includes anionic, cationic and non-ionic surfactants) (2) polymers as dispersion aids; (3) direct dispersion of pristine or functionalized CNTs in organic solvents and water (4) other dispersion like DNA, protein or starch (L.Hu, 2010). The pH value of the surfactants decides its absorption capability on CNT surface. Also the sonication time and surfactant critical micelle concentration act as a deciding factor in the absorption. It is always preferred to achieve individual CNT for surfactant based dispersion, because the electronic performance of films highly depends on the bundling of CNTs (O .Matarredona, 2003), (M. F. Islam, 2003 ). Sonication is also very important, especially, for surfactant assisted CNT dispersion. Dispersion happens by the formation of gaps or space at the CNT bundles end in the high shear environment of the ultrasonicated solution (M.S.Strano, 2003). The adsorbed surfactants diffuse in that space along the bundle and hence separate the CNTs (H.Stahl, 2000). But we have to be careful for sonication as it can damage the CNT walls and the end portion and even can cut the tubes, resulting in dramatic decrease in conductivity (B.H.Chen, 2006).

### 3.2.3 CNT AS INTERCONNECTS

Properly rolled SWCNTs can show very high current density in the order of  $10^9$ – $10^{10}$  A/cm<sup>2</sup> (B.Q.Wei R. V., 2001). This type of property of SWCNT has opened a new dimension to scaling interconnects in nano-metric dimension. For copper, though the bulk resistivity is 1.7  $\mu\Omega$ cm, with surface scattering and cross section shrinkage, the

resistivity rises quite much higher than the original value. Presently, metallic CNT has been proposed to replace copper in nano–interconnects (Burke, 2003) (A.Naeemi, 2007). SWCNT interconnects show better performances at intermediate level. Reduction in power dissipation and high current density imply of using SWCNT bundles even for the local case (A Maffucci, Nov, 2008). The piezoresistive properties of MWCNT/polymer composite films aligned by an electric field show some interesting property (R.H.Baughman, 1999). It has been observed that application of an electrochemical voltage to a SWCNT sheet induces deformation i.e. a piezoelectric response (A.I.O. Aviles, 2011). Intrinsic coupling of electrical resistivity and mechanical deformation of CNT opens the possibilities of multifunctional properties and sensing capabilities to composite materials employing nano–structures (T.C. Theodosiou, 2010). Though electromagnetic alignment of SWCNT and MWCNT has been very successful (K. Bubke, 1997), (X. Liu, 2004) modern attempts of aligning CNTs inside a polymer matrix (E.Camponeschi, 2007) has been partially successful. It has been observed that both DC and AC electric field can induce alignment of MWCNT, and, AC fields are more efficient than DC fields (C .Park, 2006). **It is worth mentioning that utmost care must be taken when SWCNT is sustaining remarkably high current density in the order of  $10^9$  A/cm<sup>2</sup>** (Z.Yao, 2000). The current may saturate at high electric field. Some common ways for preventions are scattering mechanism and electron beam resist and etching mask, followed by metal evaporation and lift off. The electrodes are cleaned properly in fuming Nitric acid (HNO<sub>3</sub>). Subsequently, the CNTs are deposited on top of the electrodes from a suspension of SWCNTs which is ultra-sonically dispersed in dichloroethane. Even annealing for a short time of the electrodes at 180°C enhances the reproducibility of the contact resistance.

### 3.3 ELECTROTHERMAL EFFECTS IN CNT

Electro-thermal effects play an important role in the properties of metallic SWCNT in interconnection applications. Experimental results and theoretical modelling disclose that self-heating is quite significant in short nanotube ( $1 \mu\text{m} < l < 15 \mu\text{m}$ ) under high bias (W.Soliman, 2013 ). CNT offer numerous benefits compared to Cu interconnects. CNT when densely packed has higher conductivity than scaled Cu interconnects for large length (W.Soliman, 2013 ). Secondly, an isolated CNT is capable of carrying current densities in excess of  $10^{10} \text{ A/cm}^2$  without any kind of damage even at an elevated temperature of  $250^\circ \text{ C}$  (H .Li, 2008) Thirdly SWCNT are very strong as discussed above, exhibiting Young Moduli of 1–2 TPa (Q. Cao, 2009). Fourthly, the thermal conductivity of CNT is 15 times the conductivity of Cu and 2 times that of diamond which makes it quite ideal for dissipating heat from sensitive active devices (F. Kreupl, 2002). Also it is to be remembered that copper has the issue of high CTE (Co-efficient of Thermal Expansion) mismatch with silicon that leads to thermo mechanical stress which decrease the reliability of the devices. CNT is promising for its extraordinary electrical, mechanical and thermal properties and is considered as a very suitable material for electronic packaging either in the pure form or filler as composite (L.Aryasomayajula, 2013).

### 3.4 SEVERAL MACROSCOPIC RESULTS (MECHANICAL PROPERTIES)

CNT bundles have drawn adequate attention due to their density, elastic modulus and mechanical strength. It is believed that ambitious projects like space elevator and super bridges can be constructed by flourishing the unique properties of CNT (M.F.Yu, 2000). For simulating the macroscopic behaviour there are several ways, one of them is hierarchical fibre bundle model which approaches specifically to carry out multi scale simulation for CNT based cables and estimating relevant mechanical

characteristics such as Young's modulus, strength or released energy during damping progression, and evaluate the scaling of these properties with cable size (N.Pugno, 2009). In this concept, it is assumed that the end to end connections in nanotubes and nanotube bundles have strength comparable to that of nanotubes or bundles themselves, assuming a long enough overlap length. Defects in the CNT structures play a crucial role in the result of macroscopic simulation. Defects can be present in atomic level or on larger scale size when fractured CNT bundles are present. For sake of avoiding complication, uniform defects are considered along the whole structures or clustered defects which is also known as circular defects. The several important results from previous literature are listed in Table 3.1 which shows that CNT has better tensile strength than copper. Molecular dynamic simulations are used to calculate theoretically the tensile response of fibres composed of CNT with intermolecular bonds of interstitial carbon atoms. Both theoretical and experimental studies have shown that the elastic modulus of a carbon nanotube is in the range of 1–2 TPa.

As mentioned earlier, with increasing contact length, CNT loses its stiffness when macroscopic fibre is produced. It has been estimated the CNT contact length required to achieve the load transfer needed for intrinsic carbon nanotube breaking strength could be on the order of 120  $\mu\text{m}$  (D. Qian, 2002). It has been observed that including cross link atoms between the carbon nanotubes in the strands increases the load transfer between the carbon nanotubes and prevent them for slipping with an increase of elastic modulus and critical strain. Also fibres constructed with longer CNT possess maximum tensile strength with lower concentration of crosslinks. (C.F. Cornwell, 2010).

**TABLE 3.1** Different Tensile Strength findings from past research

<b>Tensile Strength (GPa)</b>	<b>Remarks</b>	<b>Reference</b>
1.2	Iodine doped SWCNT	(N.Behabtu, 2013)
0.64	DWNT	(Y. Zhao, 2011)
1.54	SWCNT double/triple walled with polyvinyl alcohol infiltrated.	(J.Jia, 2011)
4	CVD/MWCNT	(J.N. Coleman, 2006)
4.1	PEEK / SWCNT Composite	(A.M.D.Pascual, 2010)
3.9	Carbon Fibre(PAN Based)	(F. An, 2012)
1.8	CNT/ PVA	(Z. Spitalsky, 2010)
1	CNT Yarn by twisting and shrinking process	(K.Liu, 2010)
1.5	SWCNT/PVA Composite	(Q. Cheng, 2009)
0.22	Copper	(Copper Development Association Inc, 2013)

### **3.5 CNT ELECTRICAL CONDUCTIVITY–MACROSCOPIC BEHAVIOR**

Department of Mechanical Engineering, Rice University, USA and Department of Mechanical Engineering, Tsinghua University, China have developed iodine doped carbon nanotube cables in 2011 which have successfully exceeded the specific electrical conductivity of metals (Y. Zhao, 2011). In this paragraph, we will discuss the process of fabrication and the properties of this type of nano–cable in details. They have reported the fabrication of iodine doped, double-walled nanotube cables with electrical resistivity approximately  $10^{-7} \Omega\text{m}$ . Because of their low density, specific conductivity (conductivity/mass) is more than in copper and aluminium and just below that of the highest specific conductivity metal, sodium. The cable possesses high current carrying capacity of the order of  $10^4\text{--}10^5 \text{ A/cm}^2$ . Also, it can be joined together for arbitrary length and diameter without diminishing the electrical properties. The

conductivity variation of this type of nanotube cable as a function of temperature is one fifth of that copper and it can be used in application from low dimensional interconnects to transmission lines. The different conductivity from major publications along with this work is listed below in Table 3.2.

**TABLE 3.2** Different electrical conductivity findings from past researches

Year of Study	Electrical Conductivity (Scm <sup>-1</sup> )	Remarks	Reference
2005	3500	Addition of SOCl <sub>2</sub> increases the conductivity by a factor of 5 when compared to that of pristine CNT	(U.D .Wegilikowska, 2005)
2005	1.85 · 10 <sup>3</sup>	MWCNT being oxidized by mixture of H <sub>2</sub> O <sub>2</sub> and NH <sub>4</sub> OH solution giving higher conductivity	(Y.J. Kim, 2005)
2006	5 · 10 <sup>-4</sup>	35 % SWCNT loading in poly (3-octylthiophene) matrix	(E.Kymakis, 2006)
2007	10 <sup>-2</sup>	4 % CNT used in polypropylene	(S.H. Lee, 2007)
2007	592.5	CNT fibre	(Q. Li, 2007)
2007	907.4	CNT fibre coated with Au-nanoparticles	(Q. Li, 2007)
2008	0.15	4 % MWCNT used in films	(N.Grossiord, 2008)
2008	7.2 · 10 <sup>3</sup>	100 % CNT matrix without insulating layer	(C. Li, 2008)
2008	10 <sup>4</sup>	Individual CNT, more conductive because unlike percolation matrix, here contact points are less, as two straight CNT can have only one contact point.	(C. Li, 2008)
2008	16.5	Acid mixture treated CNT/PANI composite	(O.K. Park, 2009)
2008	10	2wt % CNT used in films	(N Grossiord J. L., 2008)
2009	(4.4±1.6) · 10 <sup>5</sup>	SWCNT in pristine form	(P.N. Nirmalraj, 2009)

2009	$(5.6 \pm 1.2) \cdot 10^5$	SWCNT being treated with acid, contact resistance decreased considerably	(P.N. Nirmalraj, 2009)
2009	30	30 % CNT Foam	(M.A. Worsley, 2009)
2009	5	MWCNT-PANI/Au or Ag composite	(K.R. Reddy, 2009)
2009	10	SEBS/ MWCNT composite with 15wt % MWCNT	(Y.Li, 2009)
2010	$1.35 \cdot 10^{-3}$	sPS/ MWCNT composite with 3 % MWCNT Content	(G.Sun, 2010)
2010	0.12	CNT epoxy composite with 36 wt % of CNT	(Q.P. Feng, 2010)
2010	$2 \cdot 10^2$	70 wt % nano-graphite/ graphene sample	(U. Khan, 2010)
2010	298	Graphene oxide film being kept in 55% Hydroiodic acid for 1 hour at 100 C	(S. Pei, 2010)
2010	14	Vertically aligned MWCNT 6 mm high and array density of $0.06 \text{ g cm}^{-3}$	(M.B.Jakubinek M. W., 2010)
2010	40	Bi layers of PDDA/(SWCNT+DOC) films	(Y.T. Park, 2010)
2011	850	Graphene nanosheet powder	(J. Du, 2011)
2011	1.08	10 mg/ml SWCNT	(K.H. Kim, 2011)
2011	$5 \cdot 10^3$	Raw DWNT doped with iodine	(Y. Zhao, 2011)
2012	300	MWCNT at low temperature, 300 K	(M.B.Jakubinek, 2012).
2012	$3.1 \cdot 10^4$	CNT /PAN Composite	(T. Maitra, 2012)
2013	$3.1 \cdot 10^4$	Pure CNT macroscopic wire	(N.Behabtu, 2013)
2013	$5.5 \cdot 10^4$	Iodine doped CNT macroscopic wire	(N.Behabtu, 2013)
2013	$5.57 \cdot 10^3$	PANI and 5 % CNT composite	(J. Zhu, 2012)

The carbon nanotube produced in Rice University has showed the capacity to carry four times as much electrical current as copper cables of the same mass. Though transmission of current increases approximately by a factor of 5 for individual

nanotubes when compared to that of copper, the tubes when coalesced to form a fibre failed to reach that capability. This new nanotube has been claimed ideal for lightweight power transmission in systems where low weight is required like spacecraft and aerospace applications. (Williams, 2014)

The physics behind CNT Conductivity is known as **Ballistic Conduction**. Resistivity occurs because an electron while moving in a medium is scattered by impurities, defects, the atoms/molecules composing the medium that oscillate around their equilibrium positions. Ballistic transportation is observed when the mean free path of the electron is much longer than the dimension of the medium through which the electron travels. So in CNT, the mean free path is quite much larger than in copper and other metals which could have helped it to be even super conductive, but it does not happen in that way. The higher mean free path (*a benefit for CNT*) advantage from the electrical conductivity point of view is significantly reduced for the effective density of states of nanotubes.

In traditional metals, phonons backscatter electrons through a series of small angle scattering events that eventually reverse the direction of an electron. This is not possible in a 1-D conductor such as nanotube, where only forward and backward propagation is possible. As the effective density of states in nanotubes is much lower (*which also explains why CNT is light*) than in traditional metals because of the semi metallic nature of graphene, the resulting conductivity in theory is slightly higher than in metals and not exceeding too much from the mean free path perspective. The theoretical resistivity of CNT is of the order of  $10^{-8} \Omega \text{ m}$ , which is about half of that of copper. (PL McEuen, 2002)

Upon analysis of the practical data in the previous pages, we can find the macroscopic trend of CNT over years, and can get an idea where can we reach to the **theoretical value  $10^8 \text{ S}\cdot\text{m}^{-1}$**  (PL McEuen, 2002). Fig. 3.1 shows the practical development in conductivity.

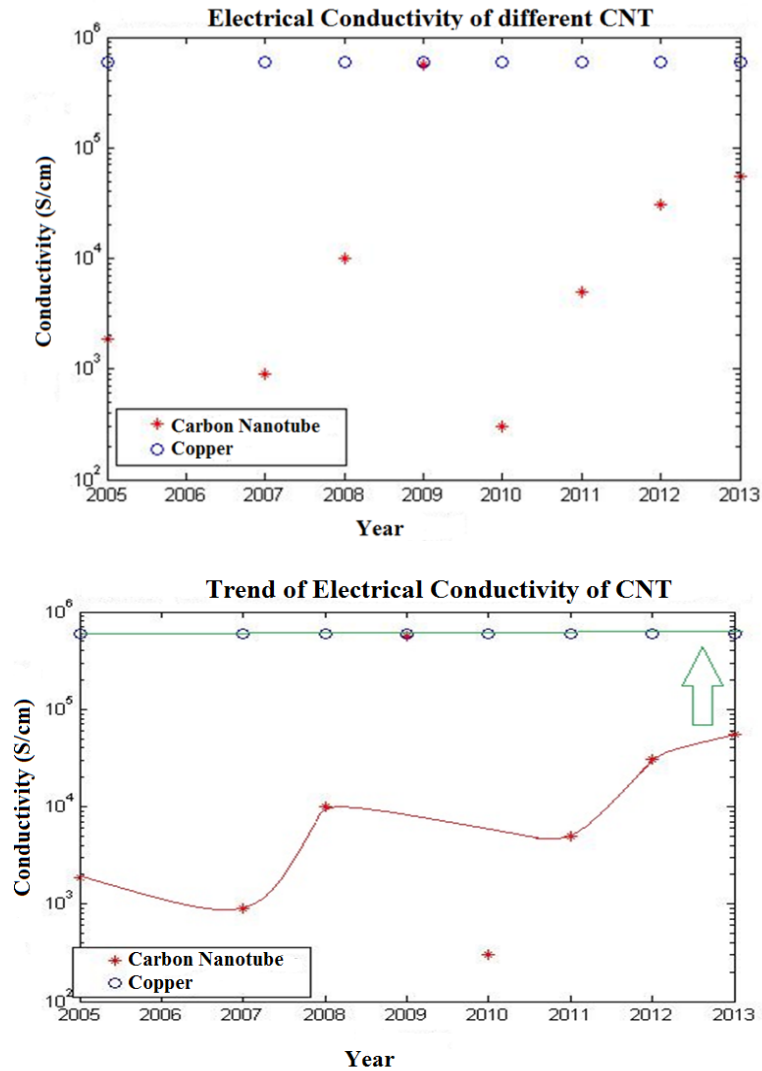


**Fig 3.1:** Development of the Electrical conductivity of CNT

In Fig 3.1, the sample of CNT in year 2009 which is showing almost equal conductivity with the conductivity of copper is actually referring to the conductivity of CNT with metallic contact (P.N. Nirmalraj, 2009). We have seen from the different analyses that the conductivity of any CNT composite is highly dependent on the amount of CNT loading. It has been observed that the best conductivity can be achieved when 100 % CNT is used to form the macroscopic wire. Fig 3.2 will give us an idea how the conductivity changes with different CNT loadings.

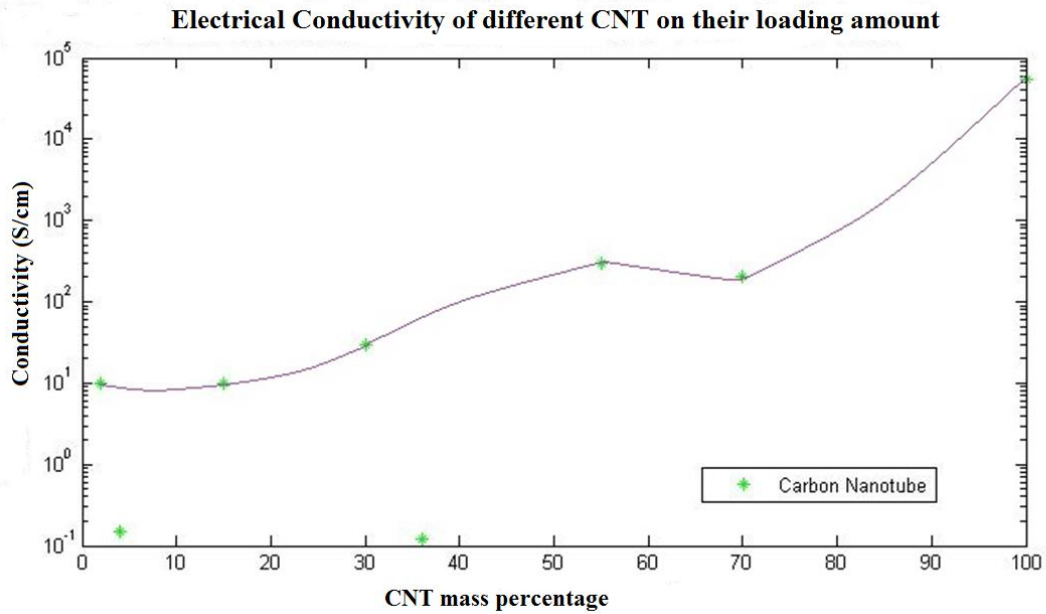


**Fig 3.2:** Electrical Conductivity of different CNT on their loading amount

The electrical conductivities of the cables are improved by iodine doping because it increases the density of mobile holes (Fischer, 2002). Though in terms of conductivity it is still lower than those of copper and aluminium, but iodine doped cable has an average density of  $0.33 \text{ g/cm}^3$ , which increases its specific conductivity to  $1.96 \cdot 10^4 \text{ Sm}^2/\text{kg}$  which is higher than in copper and aluminium but slightly lower than in sodium, Fig 3.3.

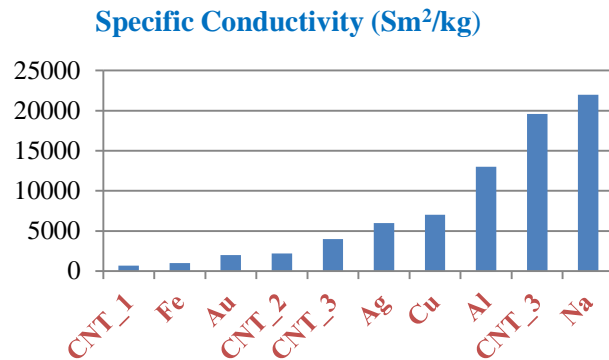


**Fig 3.3:** The Specific Conductivity of different CNT with respect to metal, CNT\_1 (K.Liu, 2010), CNT\_2 (N.Behabtu, 2013), CNT\_3 (Y. Zhao, 2011).

When compared to Cu with this DWCNT for the relative resistance (measured temperature  $R_T$  vs  $R_{300\text{ K}}$ ) in the temperature range of 200 K–400 K, the variation is quite much smaller in case of nanotube. Even prolonged usage in heated condition does not affect much the conductivity of DWCNT.

The SWCNT prepared by Tejin Aramid has shown a comprehensive stability of conductance with respect to temperature, Table 3.3. The current has been measured with varying temperature and voltage, and the resistance has not changed much, Table 3.3 and Fig 3.4. It is worth mentioning that 115° C considered as a standard temperature in the winding of medium size electric machine.

**Table 3.3** Changes of Resistance with temperature of Tejinaramid produced CNT yarn

Current	Voltage	Temperature (free in air)	Temperature (isolated)	Resistance
$I$	$U$	$T$	$T$	$R$
[A]	[V]	[°C]	[°C]	[ $\Omega$ ]
0	0	21	21	-
0.5	2.5	34	37	5
1	4.5	55	66	4.5
1.5	6.5	88	115	4.33

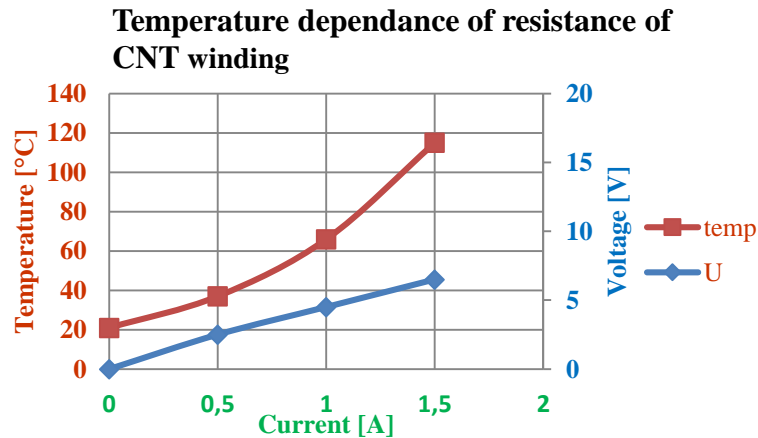


**Fig 3.4:** The change of resistance with respect to varying temperature

### 3.6 BENEFITS OF USING CARBON NANOTUBES IN ELECTRICAL MACHINES

It has been analysed in details the prospects of CNT nanotubes in the above paragraphs to replace copper as a new step towards future electrical machines. Several case studies and examples have been analysed to identify the superiority of CNT. Also special stress has been given on CNT Composites and dispersion. Now, let us analyse the property results and see how it is going to change the electrical machines. The superiority of CNT made winding for electrical machine is listed below:

a. Though right now it is not practically possible to reach the theoretical conductivity what CNT can deliver, but if it is possible in near future, it can change the whole course of electrical machine design. The resistivity of copper is  $1.67 \cdot 10^{-8} \Omega\text{m}$  at  $20^\circ\text{C}$ . Its temperature coefficient per degree C is  $3.81 \cdot 10^{-3}$  (Copper Development Association Inc, 2013). When an electrical machine is running, on an average we can consider the winding temperature to be  $120^\circ\text{C}$ . So at that temperature, the resistance of copper become around  $2.32 \cdot 10^{-8} \Omega\text{m}$ . But CNT resistance does not change with temperature. So, we can achieve 2.3 times the conductivity of copper. In the following chapter a theoretical analysis is done to showcase how much the electrical machine will be improved if we can have CNT made wiring. Without a doubt, this change will make **electrical machine either smaller in size or more efficient** than our present machines which can be the next big technological revolution. Less iron will be needed which results in less iron losses. Due to low resistance, the Joule loss will be also significantly less. So this new generation of Electrical machine will be **more efficient** than present electrical machine.

b. The specific mass of CNT is lower than that of copper and lot of other metals. This will help us to manufacture **lighter electrical machines**. Lighter electrical machines are very important for spacecraft and aeronautical sector. CNT-winding machine can enhance the space programs of different countries.

c. High current density is another big attribute of CNT. Electrical machine is intended for producing torque derived from the Lorentz force (Pyrhonen) given as

$$\sigma_{\text{Ftan}} = \frac{\hat{A}\hat{B}_\delta \cos \gamma}{2} = \frac{A\hat{B}_\delta \cos \gamma}{\sqrt{2}} \quad (3.1)$$

where  $A$  is the linear current density;  $\hat{B}_\delta$ , the peak value of the air gap normal flux density; and  $\gamma$ , the spatial angle between the flux density and linear current density distributions' fundamentals, the best angle obviously being  $\gamma = 0$ . As we can see that the variable that can be really changed is the linear current density  $A$ . Incorporation of carbon nanotube which has higher current density in the range of  $10^{10}$  A/m<sup>2</sup> (copper is only in the range of  $4 \cdot 10^6$  A/m<sup>2</sup>) can significantly change the machine design, application, controls etc. Because of the nanoscale cross-section of an armchair nanotube, electrons propagate only along the tube's axis and electron transport involves quantum effects. Carbon nanotubes are referred to as one-dimensional conductors. In electrical machines such one-dimensionality should be just a benefit as it should make **eddy currents practically irrelevant**. As the eddy current loss will be minimal in case of carbon wire made machine, the design of slots can be changed.

d. Chile, Indonesia, USA, Australia, China and Canada have the major deposits of copper. The production around the globe is 12 million tons every year, and the exploitable reserves are around 300 million tons which is expected to serve us for the next 25 years. Though 2 million tons of copper are recycled every year, eventually we are going to face scarcity. Now, CNT is nothing but carbon allotrope which is highly abundant everywhere in the world. Once CNT will become a viable option and can be used in machines, the mass production cost will be quite much lower. The fabrication cost has potential to become lower than the production cost of copper. Electrical machines will eventually be **cheaper**.

e. Though recycling of both CNT and copper is good, copper still has a higher environmental impact than CNT. Copper can act detrimental for the activity in soils, and it affects the activity of micro-organism and earthworms. The decomposition of

organic compounds can become slow due the presence of copper in soil whereas CNT is, at least in principle, very environmental friendly. CNT wound electrical machines will be quite **harmless** to the environment after their service period is over.

f. We have seen in the previous discussion that CNT is highly corrosion resistant. It can bring a great attribute to the electrical machine. In presence of acidic, moisture environment, copper can show a degrading behaviour which affects the machine performance. But CNT made winding will act quite proficiently in harsh condition.

In the following chapter, we will see how the electrical machine design is changed when we consider the winding is made of CNT. The analysis is done on the theoretical conductivity of CNT. The design changes and benefits for electrical machine have been presented analytically.

## 4. MACHINE DESIGN ANALYSIS

It is expected that there is a future possibility that CNT-based conductors can significantly change the design of electrical motors and generators. In this chapter, the changes when the machine winding is changed from copper to theoretically conductive CNT conductors have been analysed. Four types of machines have been considered for the analysis purpose: 10 kW permanent magnet synchronous motor (PMSM), 25 kW PMSM, 150 kW PMSM and 1 MW permanent magnet synchronous generator (PMSG).

### 4.1 BASIC DESIGN PROCEDURES

The design procedure for rotating electrical machines is in accordance with the reference (Pyrhonen, Design of rotating electrical machine, 2008). The design normally starts by defining the required parameters for the machine.

- Rated Power  $P$ , [W]
- Rated speed  $n$ , [rpm]
- Nominal line to line voltage  $U$ , [V]
- Desired power factor  $\cos\varphi$
- Number of phases  $m$
- Estimated efficiency  $\eta$
- Desired tangential stress  $\sigma_{Ftan}$ , [Pa]
- Maximum speed being defined by the field weakening range
- Overload capability and maximum torque at low speeds

A high value of tangential stress signifies high magnetic and electric loadings on the electrical machine and vice versa. In practice, high magnetic loading implies that the

machine must have magnets with high remanence. High electric loading means that a high value of current is injected into the machine, thereby leading to a high current density and intensive cooling. For a radial flux machine, a certain rotor volume  $V_r$  is needed to satisfy the desired tangential stress, as given by the following equation.

$$V_r = \frac{T_r}{2\sigma_{Ftan}} = \frac{60P}{4\pi n\sigma_{Ftan}} \quad (4.1)$$

where  $T_r$  is the required torque.

#### 4.1.1 ROTOR DIMENSIONING

In a radial flux machine, the rotor diameter  $D_r$  can be empirically obtained by the following equations:

$$\chi = \frac{\pi}{4p} \sqrt{p} \quad (4.2)$$

$$D_r = \sqrt[3]{\frac{4V_r}{\chi\pi}} \quad (4.3)$$

where  $\chi$  is the ratio of equivalent core length and air-gap diameter,  $p$  is the number of pole pairs.

It is possible to select slightly different dimensions from the optimum dimension since it does not change the machine properties considerably, especially in case of permanent magnet synchronous machine. Hence, the rotor diameter  $D_r$  can be chosen with a wider range. If the machine has a long spindle rotor with a small diameter, it is suitable for high speed machines. On the contrary, if the machine has a big diameter with a short stack, it is more suitable for direct drive high torque machines and different integrated applications.

With short stacks, the leakage inductance can be higher leading to lower maximum torque. Moreover, the bigger diameter will increase the length of the end winding lead and cause more end winding leakage and copper losses. In the analysis of the

machines, the diameter has been calculated with Equation (4.3). After the selection of diameter, the length of the rotor is calculated as

$$l' = \frac{4 V_r}{\pi D_r^2} \quad (4.4)$$

The stator core length  $l$  can be calculated as

$$l = l' - 2\delta \quad (4.5)$$

where  $\delta$  is the length of the airgap. One has to remember that the rotor magnets must then be longer than the stator.

The inner stator diameter  $D_s$  is calculated as

$$D_s = D_r + 2\delta. \quad (4.6)$$

#### 4.1.2 ELECTROMAGNETIC DESIGN OF STATOR AND ROTOR

The first step for the electromagnetic design of the stator is the selection of the peak value of the fundamental flux density harmonic in the air-gap,  $B_{1\text{peak}}$ . In the case of permanent magnet synchronous machine, due to the saturation of iron and limited range of remanence of the permanent magnets, the flux density in the air-gap is chosen in the range of 0.8–1.05 T.

In the analysis of the machines, the magnets are considered as rectangular. Hence, it produces rectangular flux density in the air-gap. The rectangular flux density  $B'_{\text{max}}$  in the air gap is calculated so that it is able to produce the fundamental flux density  $B_{1\text{peak}}$  in the air gap. It depends on the selection of the effective relative magnet width  $\alpha$  and is given as

$$B'_{\text{max}} = \frac{\pi B_{1\text{peak}}}{4 \sin \frac{\alpha\pi}{2}} \quad (4.7)$$

Next, the number of coil turns in a phase winding, which are in a series connection, is calculated. The coil turns depends on the back EMF,  $E_{PM}$ , of the machine. It can vary slightly with the rated phase voltage as

$$E_{PM} = k_{ratio} U_{ph} = \frac{k_{ratio} U}{\sqrt{3}} \quad (4.8)$$

where  $k_{ratio} = 0.8-1.2$  in this analysis.

The number of coil turns in a phase winding is determined as

$$N_{ph} = \frac{\sqrt{2E_{PM}}}{\omega k_w \alpha B_{max} \tau_p l'} \quad (4.9)$$

where  $\omega$  is the electrical angular speed,  $k_w$  is the winding pitch factor,  $\tau_p$  is the pole pitch.

Next, the number of phase winding  $N_{ph}$  obtained is distributed according to the selected winding layout in  $Q_s$  slots. If  $z_Q$  is the number of conductors in one slot of an integral slot double layer winding, then  $z_Q$  must be even and integer given as

$$z_Q = \text{round}_{\text{evenint}}(z_{Qsnon}) = \text{round}_{\text{evenint}}\left(\frac{2amN_{ph}}{Q_s}\right) \quad (4.10)$$

where  $a$  is the number of parallel branches in the phase winding. The number coil turns per phase is corrected according to rounded of and even  $z_Q$ , and the corrected rectangular flux density in the air-gap,  $B_{max}$ , is given as

$$B_{max} = \frac{z_{Qsnon}}{z_Q} B'_{max} \quad (4.11)$$

After the selection of the flux density in the air gap, the flux densities over the remaining parts of the magnetic circuit, like the teeth, stator yoke and rotor yoke are chosen. Higher value of flux density increases the power density and torque of the machine. But too high flux density leads to oversaturation which increases the leakage inductances. The efficiency will be decreased with higher losses resulting in excess heating. One optimal solution is to select the flux density for higher torque machine to the value where iron material just starts to saturate. Hence, selection of flux

densities is an optimum choice between weight, efficiency, performance and price of the machine. The flux densities for different parts of permanent magnet synchronous machines are given by Table 4.1. (Pyrhonen, Design of rotating electrical machine, 2008)

**Table 4.1** Flux densities in a Permanent Magnet Synchronous Machine

Part of the Machine	Flux density [T]
Air gap, $B_{1\text{peak}}$	0.8 – 1.05
Stator yoke, $B_{\text{ys}}$	1.0 – 1.5
Rotor yoke, $B_{\text{yr}}$	1.3 – 1.6
Tooth, $B_{\text{dapp}}$	1.5 – 2.0

In the calculation of this analysis, the flux densities have been chosen as per Table 4.2 for different of permanent magnet synchronous machines.

**Table 4.2** Flux densities in 10 kW, 25 kW, 150 kW, 1 MW permanent magnet synchronous machines

Part of the Machine	10 kW Flux density [T]	25 kW Flux density [T]	150 kW Flux density [T]	1 MW Flux density [T]
Air gap, $B_{1\text{peak}}$	0.95	0.96	0.91	1.05
Stator yoke, $B_{\text{ys}}$	1.5	1.41	1.2	1.3
Rotor yoke, $B_{\text{yr}}$	1.5	1.5	1.5	1.6
Tooth, $B_{\text{dapp}}$	1.6	1.6	1.6	1.5

The above mentioned values are selected for the optimum level in the magnetic field strength before saturation. The machine normally has higher magnetic flux density in the tooth due to the armature reaction. After the selection of the apparent tooth flux density, the tooth width is calculated as

$$b_d = \frac{l' \tau_u B_{\text{max}}}{k_{\text{Fe}} l_s B_{\text{dapp}}} \quad (4.12)$$

where  $B_{dapp}$  is the apparent tooth flux density,  $b_d$  is the tooth width.

The slots for the PMSMs, 10 kW, 25 kW and 150 kW in this analysis have been selected according to Fig 4.1.

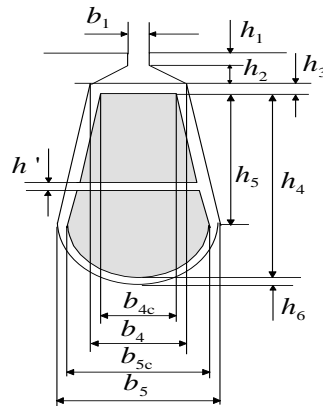


**Fig 4.1:** Stator slot for the permanent magnet synchronous motor (PMSM) 10 kW, 25 kW, 150 kW. (Pyrhonen, Design of rotating electrical machine, 2008)

In the calculation of the motors, the dimensions for the slots are chosen as given below, Table 4.3.

**Table 4.3** Dimensions of slots

Slot parameters (mm)	10 kW	25 kW	150 kW
$b_1$	3	3	4
$h_1$	1	1	5
$h_2$	2	0.5	1
$h_3$	5	1	5
$h_6$	0.5	1	1
$h'$	0.5	0.5	0.5

The value of  $h_4$  is calculated after the calculation of total cross sectional area for the winding material in the slot,  $S_{CuS}$  which is given as

$$S_{\text{CuS}} = \frac{z_Q S_{\text{cs}}}{k_{\text{Cu}}} = \frac{z_Q}{k_{\text{Cu}} I_s a J_s} \quad (4.13)$$

where  $z_Q$  is the number of conductors in one slot,  $S_{\text{cs}}$  is the area of winding material carrying current,  $k_{\text{Cu}}$  is the winding material space factor, in this calculation it is about 0.63,  $J_s$  is the desired current density. The stator current  $I_s$  is calculated with the expected efficiency and power factor. The stator current  $I_s$  is given as

$$I_s = \frac{P}{m \eta U_{\text{ph}} \cos \varphi} \quad (4.14)$$

The value of current density,  $J_s$  is an optimum choice between efficiency, heating and size of machine. The slot for the permanent magnet synchronous generator is selected as Fig 4.2

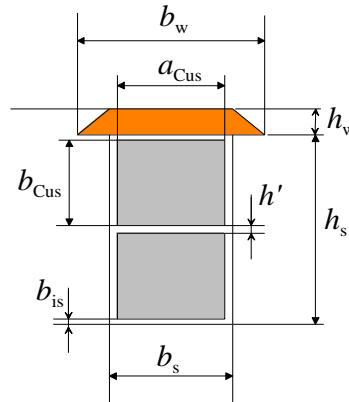


**Fig 4.2:** Stator slot for the permanent magnet synchronous generator, 1 MW. (Pyrhonen, Design of rotating electrical machine, 2008)

The different slot dimensions are given in Table 4.4. The value of  $h_s$  is calculated after calculating current carrying copper slot which is given by Equation (4.13). After that, same procedure is followed as Equation (4.14). The winding space factor  $k_{\text{Cu}}$  is 0.5 in this generator analysis.

**Table 4.4** Different Slot dimensions

Different Slot dimensions (mm)	1 MW
$h'$	0.5
$b_{is}$	0.5
$b_w$	31
$b_s$	27
$h_w$	8.1

After the selection of maximum flux densities of the stator and rotor yokes according to Table 4.2, the stator and rotor yoke height is calculated as follows

$$h_{ys} = \frac{\phi_m}{2k_{Fe}(l-n_v b_v)B_{ys}} \quad (4.15)$$

$$h_{yr} = \frac{\phi_m}{2k_{Fe}(l-n_v b_v)B_{yr}} \quad (4.16)$$

where  $l$  is the length of the core with no cooling channels,  $n_v$  is number of cooling channels,  $b_v$  is the width of cooling channels,  $k_{Fe}$  is the space factor of stator core,  $\phi_m$  is the flux in the air-gap created by permanent magnet,  $B_{ys}$  and  $B_{yr}$  is the maximum flux density in the stator and rotor yokes respectively.

The height of permanent magnet is calculated as follows

$$h_{PM} = \frac{U_{m\delta e} + U_{mds} + \frac{U_{mys}}{2} + \frac{\pi c_r H_{y\max r} (D_r - h_{yr})}{4p}}{H_c - \frac{H_c}{B_r} B_{PM} + \frac{\pi c_r H_{y\max r}}{2p}} \quad (4.17)$$

where  $U_{m\delta e}$ ,  $U_{mds}$ ,  $U_{mys}$  are the magnetic voltage over air-gap, tooth and stator yoke respectively,  $H_{y\max r}$  is the maximum field strength in rotor,  $c_r$  is the correction factor.

### 4.1.3 ANALYTICAL PERFORMANCE ESTIMATION

The load angle curve can be calculated ignoring the resistive voltage drop in the stator winding and the changes of values in the synchronous inductances for saturation. The torque is calculated as follows

$$T = 3 \frac{p}{\omega} \left[ \frac{U_{\text{ph}} E_{\text{PM}}}{X_d} \sin \delta + \frac{U_{\text{ph}}^2 (X_d - X_q)}{2X_d X_q} \sin 2\delta \right] \quad (4.18)$$

where  $p$  is the number of pole pairs,  $\omega$  is the electrical angular speed,  $U_{\text{ph}}$  is the phase voltage,  $E_{\text{PM}}$  is the back EMF of one phase,  $X_d$  and  $X_q$  are direct axes reactance and quadrature axis reactance,  $\delta$  is the load angle.

The several losses in the machine which have been calculated in this analysis are Joule loss  $P_{\text{Cu}}$ , iron loss  $P_{\text{Fe}}$ , radial loss  $P_{\text{Rad}}$ , mechanical loss  $P_{\text{Mech}}$  and additional loss  $P_{\text{ex}}$ . The efficiency has been calculated as

$$\eta = \frac{P_{\text{out}}}{P_{\text{in}}} = \frac{P_{\text{in}} - P_{\text{Cu}} - P_{\text{Fe}} - P_{\text{Rad}} - P_{\text{ex}}}{P_{\text{in}}} \quad (4.19)$$

## 4.2 CARBON NANOTUBE WINDING PMSM, 10 kW

The PMSM is a three-phase permanent magnet motor with rotor surface magnets, a two-layer integral slot winding and open-circuit cooling. The initial data of the motor is as per the following Table 4.5.

**Table 4.5** Different parameters of PMSM, 10 kW

<b>Parameters</b>	<b>Values</b>
Shaft power, W	10000
Speed, 1/s ( $\text{min}^{-1}$ )	3000
Torque $T = P/(\Omega)$ , Nm	31.83
Line-to-line voltage, V star connected	120
Number of phases	3
Number of pole pairs	3
Frequency, Hz	150
Desired efficiency	0.95
Power factor ( $\cos \phi$ )	0.91
Coercivity of the permanent magnets, A/m	800000
Remanent flux density of the permanent magnets, T	1.05
Relative permeability of the permanent magnet material	1.05
Temperature rise in the machine windings, °C	80
Space factor of the stator core	0.97
Density of iron, $\text{kg/m}^3$	7600
Density of the permanent magnet material, $\text{kg/m}^3$	7500
Number of turns	18
Number of stator slots	18
Active length of core, mm	120

The values of copper winding parameter are changed as follows when copper is replaced by CNT winding according to Table 4.6.

**Table 4.6** Winding parameters of copper and carbon nanotube

<b>Parameters</b>	<b>Values for copper</b>	<b>Values for CNT</b>
Conductivity of winding material at 20 degrees C, S/m	$57 \cdot 10^6$	$86 \cdot 10^6$
Temperature coefficient of resistivity for winding material, 1/K	$3.81 \cdot 10^{-3}$	$-1.6 \cdot 10^{-3}$
Density of winding material, kg/m <sup>3</sup>	8960	1400 (msu.edu, 2014)

The analysis has been done on the following basis:

- a. Original copper winding machine which is referred as 10 kW<sub>1</sub>
- b. Copper wire has been replaced by CNT-based wire, and the main dimension of the original motor is kept same, to see how much more efficient machine we can achieve. It is referred as 10 kW<sub>2</sub>
- c. Copper wire has been replaced by CNT-based wire, and the machine is optimized with the original motor (10 kW<sub>1</sub>) efficiency, so that we can understand how small the machine can be built with the same efficiency. It is referred as 10 kW<sub>3</sub>.
- d. CNT-based wire has replaced the copper wire, and the machine is optimized with the same Joule loss as in the original motor. The original current density in winding is 4.5 A/mm<sup>2</sup> for copper winding. Since at 100 °C the conductivity of CNT is twice that of copper, the current density in winding has been considered as 10.5 A/mm<sup>2</sup> and then the machine is optimized to see how more efficient and smaller the machine can be with the same amount of Joule loss in the winding. It is referred as 10 kW<sub>4</sub>.

Table 4.7 gives us the comprehensive values of different motor parameters to understand how the machine design will change by the application of CNTs as winding material instead of copper. The pole geometry is shown in Fig 4.3.

**Table 4.7** Comparative studies of different PMSM

Parameters	Values			
	10 kW_1	10 kW_2	10 kW_3	10 kW_4
Total slot area (mm <sup>2</sup> )	310	310	155	169
Height of slot (mm)	31.3	31.3	19.5	20.7
Efficiency (%)	94	95.3	94.1	94.5
Power factor ( $\cos \varphi$ )	0.95	0.96	0.96	0.96
Load angle $\delta$ (°)	29.8	29	26.6	26.7
Stator Current (A)	112	109	111	110
Joule Loss (W)	265	111	313	264
Iron Loss (W)	140	140	87.6	92.8
Permanent Magnet Eddy Current Loss (W)	165	165	163	163
Mechanical Loss (W)	18.2	18.2	18.2	18.2
Additional Loss (W)	50	50	50	50
Resistance of a phase winding ( $\Omega$ )	$7.03 \cdot 10^{-3}$	$3.11 \cdot 10^{-3}$	$8.31 \cdot 10^{-3}$	$7.27 \cdot 10^{-3}$
Height of Permanent magnet (mm)	5.81	5.81	5.70	5.72
Magnet segment width (mm)	34.8	34.8	34.8	34.8
External stator diameter (mm)	162	162	138	140
Rotor diameter including magnet (mm)	80	80	80	80
Diameter of stator yoke (mm)	153	153	130	132
Diameter of rotor yoke (mm)	59	59	60	60.1
Mass of permanent magnet (kg)	0.97	0.97	0.95	0.96
Mass of winding material (kg)	7.99	1.25	0.47	0.54
Total active mass of the machine (kg)	18.7	12	8.79	9.09

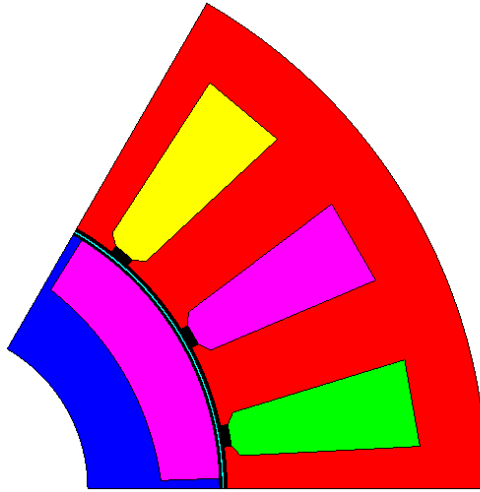


**Fig 4.3:** Pole geometry in finite element program Cedrat's Flux 2D for 10kW\_1.

The conjectures for the above analysis are

- a. If higher efficiency is needed, without compromising much on the geometry of the machine, it is possible to achieve approximately 1.5 % more efficient machine which can be considered as a significant improvement. The machine in this case will have 36 % reduced weight compared to the original copper winding machine. The Joule loss is decreased by a factor of 0.58 of that of the original copper made machine. So, the machine will be cooler than the original one. It signifies a longer life period of the machine.
- b. If exactly same efficiency machine is built with CNT replacing copper, we can reduce the size of the machine considerably, by approximately 14 % in diameter when the machine is built in the order of 10 kW. Also, the total mass of the machine can be reduced by approximately 50 % which will be a great achievement, especially in portable applications. But the only constraint is the heating of the machine. If we just consider about the winding, the Joule loss has increased by approximately 18 %. So we need to find a new set of thermal insulation for the winding. So setting a new standard for insulation will be one big change if we incorporate CNT in the winding.
- c. If same amount of Joule loss in the winding of CNT made machine is expected as in copper winding machine, it is possible to get slightly more efficient, lighter and

smaller size machine. The current density is considered as  $10.5 \text{ A/mm}^2$ . Approximately the machine will have 0.76 % higher efficiency, 48 % reduced mass and 10 % less in diameter compared to the original copper winding machine.

d. In the above calculation and the following calculations of the machines in this chapter, exact analysis for eddy current has not been performed for the application of CNT. Due to CNT's single dimensional structural nature, eddy currents will be minimal compared to copper wound machines. So a new set of calculation is needed for the exact analysis of eddy current loss in CNT wound machines. In this chapter, the calculations have been done based on the conventional eddy current analysis for copper. So, practically we can achieve even a little bit more efficient and cooler machine as stated above. The density of CNT is very low which is a major reason that CNT made machine have low mass. But, there is not much clear idea about the density of the macroscopic CNT wire which will have two times the conductivity of copper to the knowledge of the author during the writing of this thesis. The value of the density has been taken from regular CNT sample.

e. One of the biggest benefits of using CNT wire as a winding material is that even with extra heating in the winding, the conductivity of the winding is not reduced, rather it can even increase slightly. This is another reason that CNT made machines should be so efficient.

### **4.3 CARBON NANOTUBE WINDING PMSM, 25 kW**

The PMSM is three-phase permanent magnet motor with two layers of embedded magnets laminated in the rotor construction, resulting in some inverse saliency. Single layer integral slot winding has been chosen for creating additional torque. The motor has been built in the 'Laboratory of electrical drives, LUT' (J. Nerg, 2012). The initial data of the motor is as per the following Table 4.8.

**Table 4.8** Different parameters of PMSM, 25 kW

<b>Parameters</b>	<b>Values</b>
Shaft power, W	25000
Speed, 1/s ( $\text{min}^{-1}$ )	1000
Torque $T = P/(\Omega)$ , Nm	239
Line-to-line voltage, V star connected	165.4
Number of phases	3
Number of pole pairs	8
Frequency, Hz	133.33
Desired efficiency	0.95
Power factor ( $\cos \phi$ )	0.91
Coercivity of the permanent magnets, A/m	871000
Remanent flux density of the permanent magnets, T	1.15
Relative permeability of the permanent magnet material	1.05
Temperature rise in the machine windings, °C	80
Space factor of the stator core	0.97
Density of iron, $\text{kg/m}^3$	7600
Density of the permanent magnet material, $\text{kg/m}^3$	7500
Number of turns	64
Number of stator slots	48
Active length of core, mm	65

The values of copper winding parameter are changed considering that copper is replaced by CNT winding according to Table 4.6. The pole geometry is shown in Fig 4.4.

The analysis has been done on the following basis:

- a. Original copper winding machine is referred as 25 kW\_1 which has been designed similarly with the model presented in the reference (J. Nerg, 2012).
- b. Copper wire has been replaced by CNT-based yarn, and the main dimensions of the original motor are kept the same, to see how much more efficient machine we can achieve. It is referred as 25 kW\_2
- c. Copper wire has been replaced by CNT-based yarn, and the machine is optimized with the original motor (25 kW\_1) efficiency, so that we can understand how small the machine can be built. It is referred as 25 kW\_3.
- d. CNT-based wire has replaced the copper wire, and the machine is optimized with the same Joule loss of original motor. The original current density in winding is  $4.5 \text{ A/mm}^2$  for copper winding. Since at  $100^\circ\text{C}$  the conductivity of CNT is twice that of copper, the current density in winding has been considered as  $8.9 \text{ A/mm}^2$  and then the machine is optimized to see how much more efficient and smaller a machine can be with the same amount of Joule loss. It is referred as 25 kW\_4.

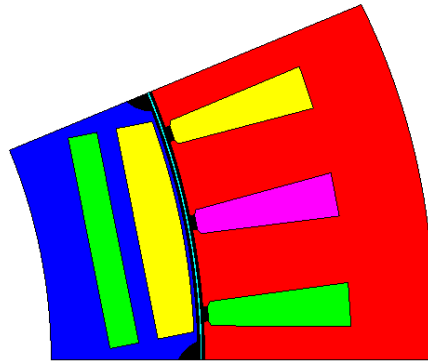


**Fig 4.4:** Pole geometry in finite element program Cedrat's Flux 2D for 25kW\_1.

In the rotor there are two embedded magnets under one pole. The construction is similar to permanent magnet assisted synchronous reluctance machine but without the flux barrier. In Table 4.9, only the total height of the two permanent magnets has been provided. Table 4.9 give us the comprehensive values of different motor parameters to understand how the machine design will change by the application of CNT.

**Table 4.9** Comparative studies of different PMSMs

Parameters	Values			
	25 kW_1	25 kW_2	25 kW_3	25 kW_4
Total slot area (mm <sup>2</sup> )	232	232	151	161
Height of slot(mm)	29.4	29.4	20.9	21.9
Efficiency (%)	95.9	96.9	95.9	96.1
Power factor (cos $\varphi$ )	0.92	0.92	0.9	0.9
Load angle $\delta$ (°)	21.5	21.3	20.1	20.2
Stator Current (A)	100	98	101	101
Joule Loss (W)	636	370	700	635
Iron Loss (W)	296	296	233	241
Mechanical Loss (W)	60.4	60.4	60.4	60.4
Additional Loss (W)	75	75	75	75
Resistance of a phase winding ( $\Omega$ )	0.02	0.01	0.03	0.02
Height of Permanent magnet (mm)	8.3	8.3	8.22	8.23
Magnet segment width (mm)	46.2	46.2	46.2	46.2
External stator diameter (mm)	380	380	363	365
Rotor diameter including magnet (mm)	284	284	284	284
Diameter of stator yoke (mm)	363	363	346	348
Diameter of rotor yoke (mm)	252	252	252	252
Mass of permanent magnet (kg)	2.76	2.76	2.73	2.73
Mass of winding material (kg)	18.7	2.90	1.63	1.79
Total active mass of the machine (kg)	44.4	28.7	24.6	25.1

The conjectures from the above analysis are as follows-

- a. When copper winding is changed to CNT-based winding without changing the geometry, we achieve 1.03 % improvement in the efficiency which is a considerable amount of improvement. Also the Joule loss is reduced by 42.35 % which indicates a

cooler machine. Even for the same geometry, due to the light weight of CNT, the machine will be lighter; approximately 35.41 % weight will be reduced.

b. When copper winding is changed to CNT-based winding and if the machine is optimized with same efficiency as copper made machine, a significant reduction in the motor dimension and weight is possible. The external stator diameter will be reduced approximately by 4.47 % and the weight of the machine will be reduced approximately by 44.61 %. The Joule loss is increased by 9.9 % and the iron loss in this case reduced approximately by 21.55 %.

c. When the CNT winding machine is optimized with the same amount of Joule loss as with copper winding machine, we can achieve higher efficiency, smaller size and reduced weight. The current density has been considered as  $8.9 \text{ A/mm}^2$  in the slot. The CNT winding machine will be 0.21 % more efficient, have 3.9 % reduced external diameter and have 43.44 % reduced weight.

### **4.3 CARBON NANOTUBE WINDING PMSM, 150 kW**

The PMSM is three-phase permanent magnet motor with embedded magnets, have a two-layer integral slot winding and water cooling. This is a traction motor built in the ‘Laboratory of electrical drives, LUT’ for using in a hybrid bus. The initial data of the motor is as per the following Table 4.10.

**Table 4.10** Different parameters of PMSM, 150 kW

<b>Parameters</b>	<b>Values</b>
Shaft power, W	150000
Speed, 1/s ( $\text{min}^{-1}$ )	2241
Torque $T = P/(\Omega)$ , Nm	639
Line-to-line voltage, V star connected	440
Number of phases	3
Number of pole pairs	8
Frequency, Hz	298.8
Desired efficiency	0.96
Power factor ( $\cos \phi$ )	1
Coercivity of the permanent magnets, A/m	871000
Remanent flux density of the permanent magnets, T	1.15
Relative permeability of the permanent magnet material	1.05
Temperature rise in the machine windings, °C	80
Space factor of the stator core	0.97
Density of iron, $\text{kg/m}^3$	7600
Density of the permanent magnet material, $\text{kg/m}^3$	7500
Number of turns	40
Number of stator slots	48
Active length of core, mm	220

The pole geometry is shown in Fig 4.5.

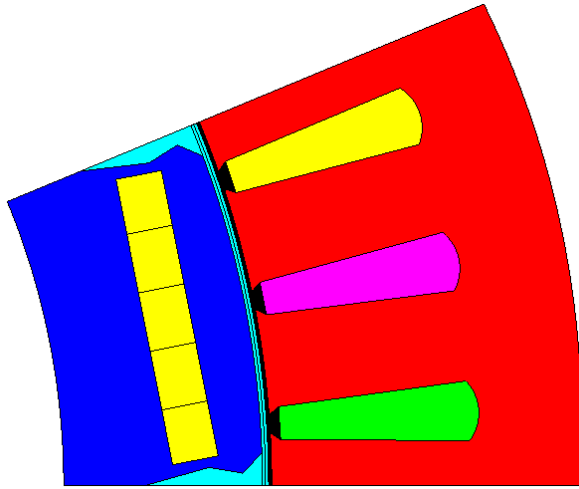


**Fig. 4.5:** Pole geometry in finite element program Cedrat's Flux 2D for 150 kW\_1.

The value of copper winding parameters are changed considering that copper is replaced by CNT winding according to Table 4.6. The analysis has been done on the following basis:

- a. Original copper winding machine which is referred as 150 kW\_1
- b. Copper wire has been replaced by CNT, and the main dimensions of the original motor are kept same, to see how much more efficient machine we can achieve. It is referred as 150 kW\_2
- c. Copper wire has been replaced by CNT, and the machine is optimized with the original motor (150 kW\_1) efficiency, so that we can understand how small the machine can be. It is referred as 150 kW\_3.
- d. CNT has been replaced the copper wire, and the machine is optimized with the same Joule loss as in the original motor. The original current density in the winding is  $4.1 \text{ A/mm}^2$  for copper winding. Since at  $100^\circ\text{C}$  the conductivity of CNT is twice that of copper, the current density in the winding has been considered as  $10.4 \text{ A/mm}^2$  and then the machine is optimized to see how much more efficient and smaller a machine can be with the same amount of winding losses. It is referred as 150 kW\_4.

Table 4.11 gives us the comprehensive values of different motor parameters to understand how the machine design will change by the application of CNT.

**Table 4.11** Comparative studies of different PMSMs

Parameters	Values			
	150 kW_1	150 kW_2	150 kW_3	150 kW_4
Total slot area (mm <sup>2</sup> )	434	434	131	203
Height of slot(mm)	47.2	47.2	19	26.9
Efficiency (%)	96.3	96.9	96.3	97.2
Power factor (cos $\varphi$ )	0.94	0.94	0.98	0.98
Load angle $\delta$ (°)	69.1	68.5	54.4	57.3
Stator Current (A)	218	216	208	207
Joule Loss (W)	$1.57 \cdot 10^3$	690	$2.41 \cdot 10^3$	$1.57 \cdot 10^3$
Iron Loss (W)	$3.26 \cdot 10^3$	$3.26 \cdot 10^3$	$1.4 \cdot 10^3$	$1.78 \cdot 10^3$
Mechanical Loss (W)	619	619	670	$1.12 \cdot 10^3$
Additional Loss (W)	300	300	300	300
Resistance of a phase winding ( $\Omega$ )	0.01	$5 \cdot 10^{-3}$	0.03	0.01
Height of Permanent magnet (mm)	6.43	6.43	6.21	6.27
Magnet segment width (mm)	39.2	39.2	39.2	39.2
External stator diameter (mm)	379	379	323	338
Rotor diameter including magnet (mm)	260	260	260	260
Diameter of stator yoke (mm)	368	368	313	328
Diameter of rotor yoke (mm)	239	239	239	239
Mass of permanent magnet (kg)	4.5	4.5	4.34	4.38
Mass of winding material (kg)	53.5	8.35	1.47	3.4
Total active mass of the machine (kg)	131	85.6	52	61.1

The conjectures from the above analysis are as follows:

- a. When copper winding is changed to CNT without changing the geometry, we can achieve a 0.57 % improvement in the efficiency. The Joule Loss of the machine will be reduced. The Joule loss is reduced by a factor of 0.56 from that of the copper winding machine. Even for the same geometry, due to the light weight of CNT, the machine will be lighter; approximately 35 % weight will be reduced.
- b. When copper winding is changed to CNT and the machine is optimized with the same efficiency as the copper made machine, a significant reduction in the motor dimension and weight is possible. The external stator diameter will be reduced approximately by 14.6 % and the weight of the machine will be reduced approximately by 60.2 %. The Joule loss is increased by 53 % and the iron loss in this case is reduced approximately by 56 %.
- c. When the CNT winding machine is optimized with the same amount of Joule loss as in the copper winding machine, we can achieve a higher efficiency, smaller size and reduced weight machine. The CNT winding machine will be 0.9 % more efficient, have 10.5 % reduced external diameter and 53.2 % reduced weight.

### **4.3 CARBON NANOTUBE WINDING PMSG, 1 MW**

The generator is a three phase permanent magnet machine with rotor surface magnets. It has a single layer, full pitch integral slot winding and open circuit cooling. The initial data of the motor is as per the following Table 4.12.

**Table 4.12** Different parameters of Permanent Magnet Synchronous Generator, 1MW

Parameters	Values
Output power, W	1000000
Speed, 1/s ( $\text{min}^{-1}$ )	300
Torque $T = P/(\Omega)$ , Nm	$3.18 \cdot 10^4$
Line-to-line voltage, V star connected	690
Number of phases	3
Number of pole pairs	10
Frequency, Hz	50
Desired efficiency	0.95
Power factor	0.98
Coercivity of the permanent magnets, A/m	800000
Remanent flux density of the permanent magnets, T	1.05
Permeability of vacuum, Vs/(Am)	$4 \cdot \pi \cdot 10^{-7}$
Permeability of the permanent magnet material	1.05
Temperature rise in the machine windings, °C	80
Space factor of the stator core	0.97
Density of iron, $\text{kg/m}^3$	7600
Density of the permanent magnet material, $\text{kg/m}^3$	7500
Number of turns	40
Number of stator slots	60
Active length of core, mm	335.7

The values of copper winding machine are changed considering that copper is replaced by CNT winding according to Table 4.6. The analysis has been done on the following basis:

- a. Original copper winding machine which is referred as 1MW\_1

b. Copper wire has been replaced by CNT, and the main dimensions of the original generator are kept the same, to see how much more efficient machine we can achieve. It is referred as 1MW\_2

c. Copper wire has been replaced by CNT, and the machine is optimized with the original generator (1MW\_1) efficiency, so that we can understand how small the machine can be. It is referred as 1MW\_3.

d. Copper wire has been replaced by CNT, and the machine is optimized with the same Joule loss of original machine. The original current density in winding is  $4.5 \text{ A/mm}^2$  for copper winding. Since at  $100^\circ\text{C}$  the conductivity of CNT is twice that of copper, the current density in the winding has been considered as  $10.3 \text{ A/mm}^2$  and then the machine is optimized to see how much more efficient and smaller machine can be built with the same amount of Joule loss. It is referred as 1 MW\_4.

The pole geometry is shown in Fig 4.6.

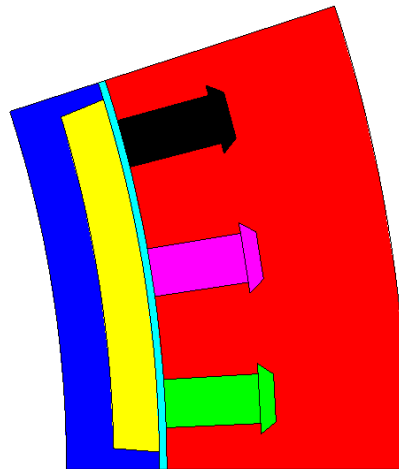


**Fig. 4.6:** Pole geometry in finite element program Cedrat's Flux 2D for 1 MW\_1.

Table 4.13 gives us the comprehensive values of different generator parameters to understand how the machine design will change by the application of CNT.

**Table 4.13** Comparative studies of different PMSGs.

Parameters	Values			
	1MW_1	1MW_2	1MW_3	1MW_4
Total slot area ( mm <sup>2</sup> )	$1.61 \cdot 10^3$	$1.61 \cdot 10^3$	584	726
Height of slot(mm)	56	56	20.4	25.3
Efficiency (%)	96.5	97.2	96.5	96.8
Power factor (cos $\varphi$ )	0.98	0.98	0.98	0.98
Load angle $\delta$ (°)	24.4	24.2	22.6	22.8
Stator Current (A)	887	880	884	881
Joule Loss (W)	$1.43 \cdot 10^4$	$6.3 \cdot 10^3$	$1.83 \cdot 10^4$	$1.45 \cdot 10^4$
Iron Loss (W)	$1.26 \cdot 10^4$	$1.26 \cdot 10^4$	$8.36 \cdot 10^3$	$8.96 \cdot 10^3$
Radial Loss(W)	$1.98 \cdot 10^3$	$1.98 \cdot 10^3$	$2.21 \cdot 10^3$	$2.17 \cdot 10^3$
Mechanical Loss (W)	$2.77 \cdot 10^3$	$2.77 \cdot 10^3$	$2.77 \cdot 10^3$	$2.77 \cdot 10^3$
Resistance of a phase winding ( $\Omega$ )	$6.15 \cdot 10^{-3}$	$2.72 \cdot 10^{-3}$	$7.87 \cdot 10^{-3}$	$6.24 \cdot 10^{-3}$
Height of Permanent magnet (mm)	20.2	20.2	19.4	19.5
External stator diameter (mm)	1610	1610	1540	1550
Rotor diameter including magnet (mm)	1350	1350	1350	1350
Mass of permanent magnet (kg)	170	170	163	164
Mass of winding material (kg)	386	59.5	20.6	26
Total active mass of the machine (kg)	$2.16 \cdot 10^3$	$1.83 \cdot 10^3$	$1.51 \cdot 10^3$	$1.55 \cdot 10^3$

The conjectures from the above analysis are as follows:

- a. Since the generator is of the order of 1 MW, a small amount of improvement in efficiency can be considered as significant. When the geometry is unchanged, and the

copper winding is replaced by CNT winding, a remarkably high improvement of 0.78 % increase in the efficiency is achieved. The Joule loss is reduced by a factor of 0.56 from that of the original copper winding machine. Also the weight is reduced by 15.2 %.

b. When the generator is optimized with the same efficiency we can achieve a significantly reduced size and weight. The external diameter is reduced by 4.4 % and the mass is reduced by 30.1 %. One of the major concerns can be the heating as the Joule loss has increased approximately by 28 % in the winding. May be new cooling system or improvement in the cooling design is needed prior using CNT in generator.

c. If we optimize the CNT machine with approximately the same Joule loss in the winding like copper made machine, we achieve improvement in efficiency as well as reduction in size and weight of the machine. The generator will be 0.32 % more efficient, have 3.82 % reduced external diameter and 28.24 % reduced weight.

In the Fig 4.7 we can understand broadly an idea that how the CNT winding is going to change the electrical machine design in future.

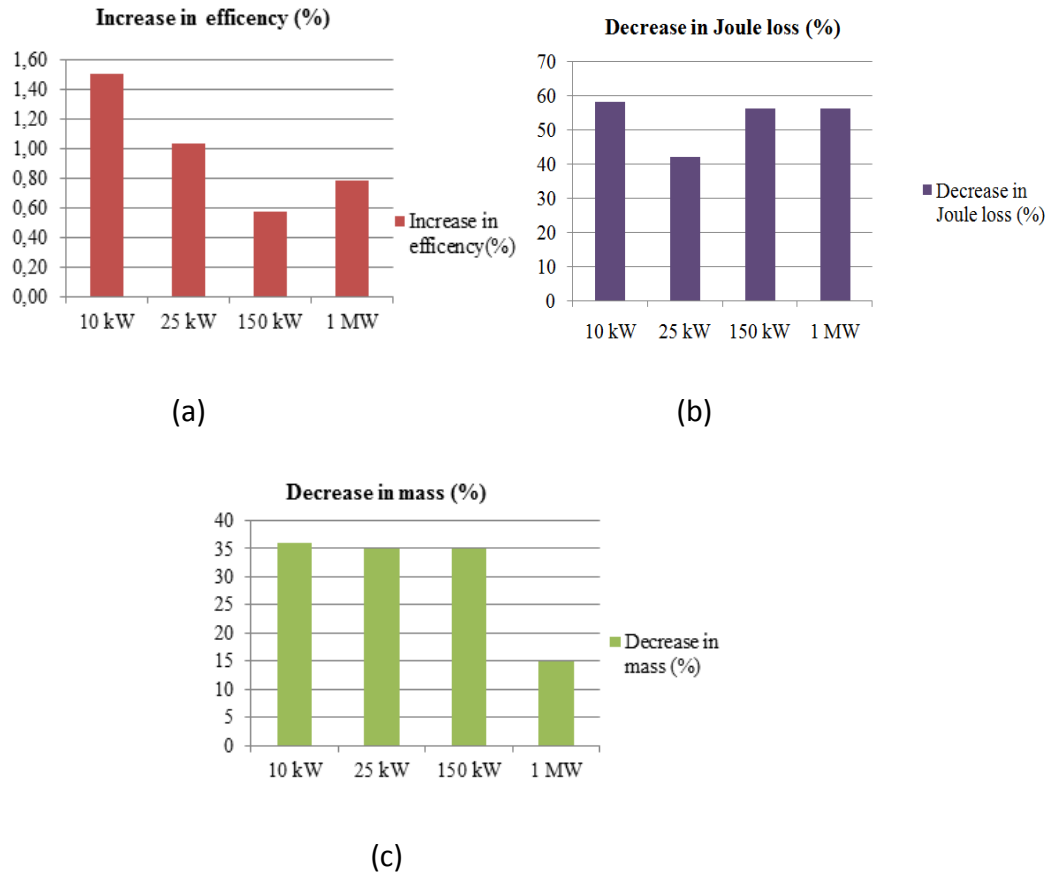


**Fig. 4.7:** A comparative chart of machine improvement when CNT winding is used instead of copper with the same geometry, (a) increase in efficiency (%), (b) decrease in Joule loss (%) and (c) decrease in mass (%)

For the same geometry, the net change of improvements is higher in smaller power rating machine. But it is only a comparative study and the improvements of the machines cannot be concluded in this manner. The changes can be different with different designs of machine and in the case of PMSMs and PMSGs, where the rotor structure plays a vital role in the behaviour of machine; the changes can be different for the same power rating.

The changes in the machines' designs are also significant when the same efficiency is obtained approximately by replacing copper winding with CNT winding, Fig 4.8.

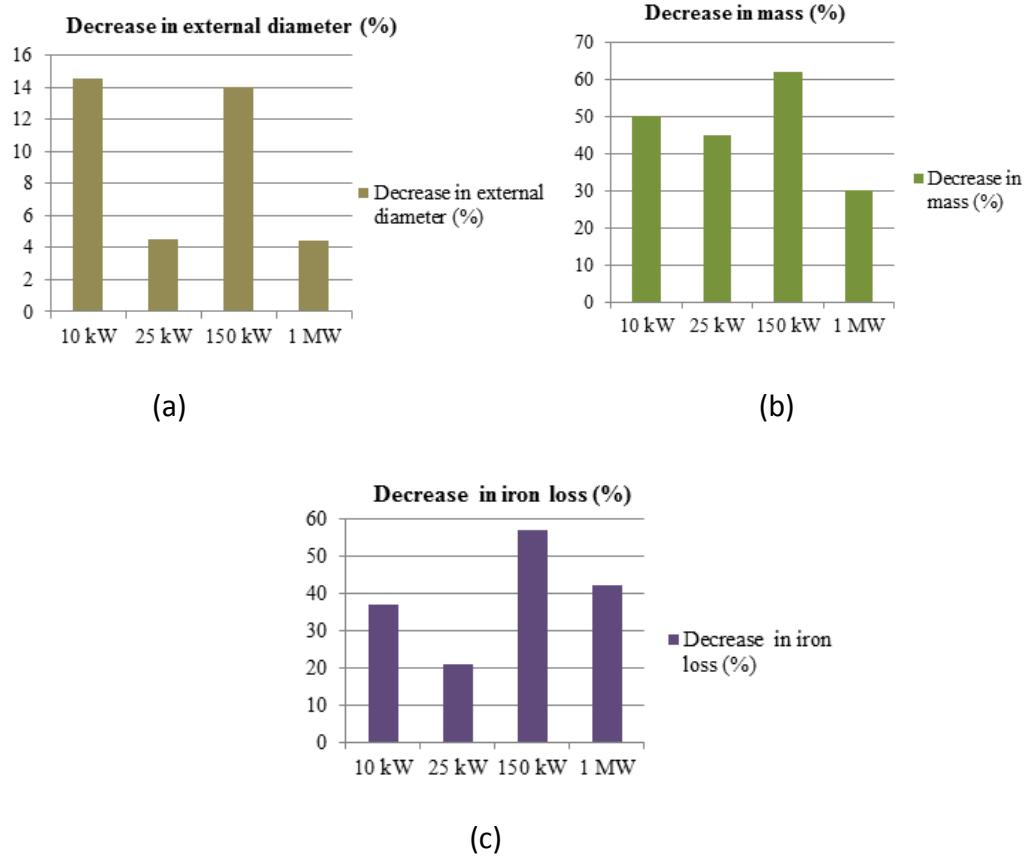


**Fig. 4.8:** A comparative chart of CNT machine improvement when CNT winding is used instead of copper winding to achieve the same efficiency in both cases, (a) decrease in external diameter (%), (b) decrease in mass (%) and (c) decrease in iron loss (%)

When the machines are optimized to have the same efficiency as the original copper winding machine, the improvements of the machine are higher with smaller power ratings. However, in the 25 kW machine, due to the special rotor construction of two layer permanent magnets which provides significant reluctance torque capability, the changes of improvement is not so big. But in general, the improvements in the machine are considerable.

The changes in the machine designs are also significant when CNT winding machines are optimized with the same amount of Joule losses as in copper winding machines, Fig 4.9.

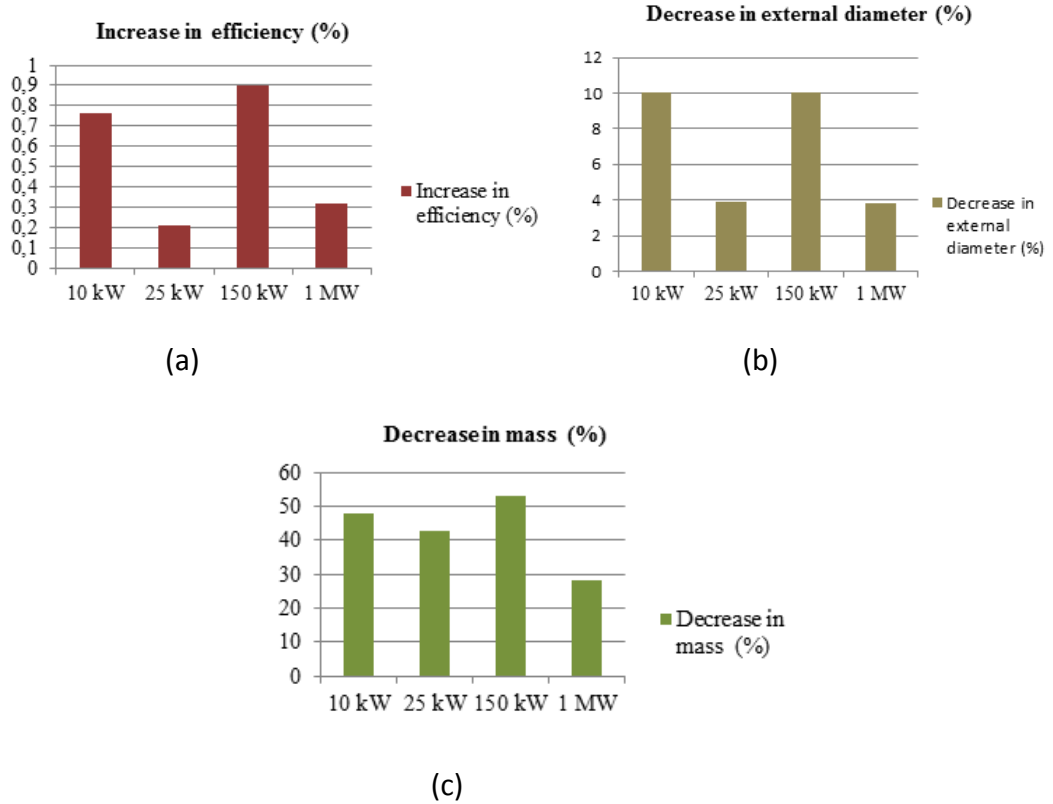


**Fig. 4.9:** A comparative chart of CNT machine improvements when CNT winding is used instead of copper and the machines have the same amount of Joule losses with the original copper winding machine, (a) increase in efficiency (%), (b) decrease in external diameter (%) and (c) decrease in mass (%)

For the same amount of Joule heating in CNT winding machine and copper winding machine, the CNT winding machines have shown considerable amount of improvements with reduced weight and size, and improved efficiency. The improvements will change with different rating and types of machines. It is very hard to predict, because for PMSMs and PMSGs, as mentioned earlier, the performances of the machine are highly dependent on the rotor construction.

## 5. CONCLUSIONS

In this thesis, new scenarios for future electrical machines are presented. After the inclusion of permanent magnet synchronous machines in electrical engineering, the next big revolution could be CNT wound electrical machines. Detailed discussions have been presented on the macroscopic properties of CNT material. Several researches have shown conclusively that over the latest decade, significant improvements have been achieved in the synthesis of CNT and retaining their properties of metallic conductivity in the macroscopic form. Several aspects of macroscopic synthesis of CNT and the improvements of the CNT wire from the manufacturing point of view have been discussed. The production of this type of CNT wire could replace the traditional metallic wire in different electrical applications including electrical machines. The CNT wire which consists of CNT fibre can now be produced with practically no limits in length and with different cross sectional areas. As the material is lighter than copper, electrical machine winding with CNT will decrease the machine weight. Several macroscopic CNTs discussed in this thesis have shown better performances than traditional copper wire. CNT wire can have significantly higher current density than copper wire which is a great attribute in reducing the size of the machine and thereby decreasing iron loss. Today, we normally use the current density in the range of  $2 - 9 \text{ A/mm}^2$  in the copper winding, which is chosen according to the heating of the insulation of the winding. Mechanically CNT wire can show better performance than the copper wire. The specific conductivity of presently available CNT wire is already higher than the copper and aluminium when the fibre is strongly doped. So we can significantly decrease the weight of the winding material in electrical machines. However, with the present CNT material, due to its high resistance and lack of proper insulation, it cannot be considered as a practically viable option. CNT wire machines can function better under harsh conditions. Copper wires degrade over years developing higher resistance, so the efficiency of a machine can decrease over years. But CNT wire shows almost no changes in resistivity under

acidic or moisture condition, which signifies that the machine performance will remain intact during its complete lifetime.

It has been shown in analytical calculations how the machine designs will be changed when CNT winding will be used in electrical machine. Modern CNT windings cannot achieve the theoretical conductivity of CNT but considering it as a future winding material forecasts a big step forward for the machine design. Theoretically, the machine size can be diminished considerably if we try to achieve the same efficiency as in a copper wound machine. It signifies that the machine will be lighter in weight than the original copper wound machine. If we replace copper windings of the machine with CNT windings, then for the same geometry of the machine, it is possible to get better efficiency and less heating. The optimization of this type of machine will be different from copper wound machine. Decreasing the size of the machine leads to increased Joule loss and decreased iron loss. Similarly, in case of CNT where the resistance is considerably low, decreasing the size can make the machine some time even more efficient than an original machine with CNT winding. Iron losses are always bigger than Joule losses when a normal machine with copper winding is replaced by CNT winding with its theoretical conductivity of  $10^8 \text{ Sm}^{-1}$ .

With a detailed theoretical analysis on different type of permanent magnet synchronous machines, it has been conclusively shown that once the theoretical conductivity of CNT is achieved through improved synthesis process, the design ideology of electrical machine will change. This type of CNT winding machine may start a new revolution in combining nanotechnology with electrical machines in the future. Since the theoretical resistivity coefficient is negative in CNT, it will be wiser to operate CNT wound machine in a higher temperature than modern day conventions. In that case, improved thermal insulation must be achieved. Also the demagnetization of the permanent magnets in permanent magnets synchronous machines can be a problem if the machine is operated in higher temperatures than the present day conventions. CNT wires are loosely attached to each other, and hence, although theoretically CNT winding can decrease slot space, windings may consume considerable amount of space due to the bulky nature of CNT wires. The winding

techniques should be changed in that case. Another problem can be the soldering of CNT wire in the end winding part. However, numerous researches are going on presently to solve the soldering issues.

The next step on this CNT winding electrical machine will be involving industrial research and development as the technology needs to be scaled up to attain the mass production capability. Significant developments are still required to increase the conductivity of the CNT wire to reach its theoretical value. Newer developments of this field rely upon the industrial and political involvement. As the current winding system and standard have been followed for more than a century with a steady infrastructure and manufacturing capability, a sudden change for using CNT wire in electrical machines must be addressed before the above-mentioned issues. It will require for the policy makers and the industrialists to understand the technology that will help to mitigate the energy crisis globally.

For future work, a detailed thermal model analysis of the electrical machine with CNT winding should be performed. The thermal conductivity of CNT is  $2000 \text{ W/(Km)}$  (M. Fujii, 2005) which is higher than in copper. Hence, the thermal behaviour in the electrical machine will be different in this case. Experimental and theoretical models need to be developed and analysed to introspect if the magnetic field put any harmful or beneficial role in the CNT winding, especially in its electrical conductivity. Also, the mechanical stability, toxic effect of CNT when used in electrical machine can be analysed vividly. Apart from CNT winding, also CNT based insulation material can be incorporated in electrical machines. CNTs can be used instead of steel in future electrical machine, since theoretically it has better strength and lighter weight than steel. Hence, mechanical stability analysis of electrical machine with CNT winding can be performed also as a future work on this subject.

## REFERENCES

- Copper Development Association Inc.* (2013). Found in [http://www.copper.org/applications/architecture/arch\\_dhb/technical-discussion/fundamentals/intro.html](http://www.copper.org/applications/architecture/arch_dhb/technical-discussion/fundamentals/intro.html)
- gizmag.* (2013). Found in <http://www.gizmag.com/threadlike-carbon-nanotube-fiber/25777/>
- Science Daily.* (2013). Found in [http://www.sciencedaily.com/articles/c/carbon\\_nanotube.htm](http://www.sciencedaily.com/articles/c/carbon_nanotube.htm)
- A Maffucci, G. M. (Nov, 2008). Performance Comparison Between Metallic Carbon Nanotube and Copper nano-Interconnects. *IEEE TRANSACTIONS ON ADVANCED PACKAGING, VOL 31, NO 4, 692-699.*
- A.I.O. Aviles, F. V. (2011). Electrical and Piezoresistive properties of multi-walled carbon nanotube/polymer composite films aligned by an electric field. *Carbon, 49, 2989-2997.*
- A.M.D.Pascual, M. N. (2010). High Performance PEEK/carbon nanotube composites compatibilized with polysulfones-II, Mechanical and Electrical properties. *Carbon (48), 3500-3511.*
- A.Naeemi, J. M. ( 2007). Design and Performance modeling for single walled carbon nanotubes as local, semiglobal and global interconnects in gigascale integrated systems. *IEEE Transaction Electron Devices, Vol 54, no 1, 26-37.*
- A.S.Deckers, B. M. (2008). In vitro investigation of oxide nanoparticle and carbon nanotube toxicity and intracellular accumulation in A549 human pneumocytes. *Toxicology 253, 137-146.*
- A.Zahab, L. P. (2000). Water vapor effect on the electrical conductivity of Single walled carbon nanotube material. *Physics review B, (62), 100000-3.*
- Abate, T. (2013). *Stanford News.* Found in <http://news.stanford.edu/news/2013/september/carbon-nanotube-computer-092513.html>
- B.H.Chen, H. L. (2006). *Applied Physics Letter, 88, 093502.*

- B.Liu, W. S. (2012). High temperature selective growth of single walled carbon nanotubes with a narrow chirality distribution from a CoPt bimetallic catalyst. *Chem Commun* 48, 2409-2411.
- B.M.Kim, A. (2004). Properties and applications of high mobility semiconducting nanotubes. *J Phys: Condens Matter* 16(18), R553-580.
- B.Peng. (2008). Measurement of near ultimate strength for multiwalled carbon nanotubes and irradiationinduced crosslinkings improvements. *Nature Nanotechnology* 3, 626.
- B.Q. Wei, R. V. (2001). Reliability and current carrying capacity of carbon nanotubes. *Applied Physics Letter, Vol 79, No 8*, 1172.
- B.S.Paratala, B. (2011). Carbon Nanotubes in Regenrative Medicine. *Carbon Nanotubes for Biomedical Applications*.
- B.T.Kelly. (1981). Physics of graphite. *Applied Science*.
- B.Vigolo. (2007). *Science* 290, 2880.
- Burke, P. (2003). An RF circuit model for carbon nanotubes. *IEEE Transaction, Nanotechnology, vol 2*, 55-58.
- C .Park, J. W. (2006). Aligned single wall carbon nanotubes polymer composite using an electric field. *Journal of Polymer Science B (44)*, 1751-62.
- C. Li, E. T. (2008). Effect of nanotube waviness on the electrical conductivity of carbon nanotube-based composites. *Composites Science and Technology (68)*, 1445-1452.
- C.F. Cornwell, J. B. (2010). *Design of very high strength alligned and interconnected carbon nanotube fibers based on molecular dynamic simulations*. IEEE computer society.
- C.Zhu, Q. R. (2005). Gas fluidization characterisitic of nano particle agglomerates. *AICHE J* 51, 426-439.
- D. Qian, G. J. (2002). Mechanics of carbon nanotube. *Applied mechanics Review* 55, 495-533.
- D.Janas, A. V. (2013). Performance of carbon natube wires in extreme condition. *Carbon*.

- D.Tomanek. (2014). *Guide through the nanocarbon jungle*. Found in IOP Science: <http://iopscience.iop.org/chapter/978-1-627-05273-3/bk978-1-627-05273-3ch1>
- D.Resaco, R.P.S. (2014). *Structure and Applications of Single-Walled Carbon Nanotubes (SWCNTs) Synthesized Using the CoMoCAT® Method*. SWENT
- E. J .Garcia, B. L. (2008). Fabrication and multifunctional properties of a hybrid laminate with aligned carbon nanotubes grown In Situ. *Composites and Science Technology* 68, 2034.
- E. Pop, D. M. (2006). Thermal conductance of an individual single wall carbon nanotube above room temperature. *Nano letter* 6, 96.
- E.Camponeschi, R. M.-H. (2007). Properties of carbon nanotube-polymer composite alligned in a magnetic field. *Carbon*, 45, 2037-2046.
- E.Kymakis, G. A. (2006). Electrical properties of single wall carbon nanotube polymer composite films. *Journal of Applied Physics* (99).
- E.W.Wong, P. C. (1997). Nanobeam mechanics: elasticity, strength and toughness of nanorods and nanotubes. *Science* 277, 1971-1975.
- F. An, C. L. (2012). Preparation and characterization of carbon nanotube-hybridized carbon fiber to reinforce epoxy composite. *Material and Design* (33), 197-202.
- F. Kreupl, A. .. (2002). *Elsevier Science, Micro Electronics Engineering*, 64, 399-408.
- F.Silly, M. (2005). Selecting the shape of supported metal nanocrystals. *Physics Review letter* 94.
- Fischer, J. (2002). Chemical doping of single walled carbon nanotubes. *Accounts of chemical research* (35), 1079-1086.
- G.D.Kiss. (2003). *Rheology and Rheo-optics of Concentrated Solutions of Helical Polypeptides*. Department of Polymer Science and Polymer Engineering, University of Massachusetts.
- G.Iannacchione, R. (2008). *Applied Physics Letter* 93, 183105.
- G.Overney, W. D. (1993). Structural rigidity and low frequency vibrational modes of long carbon tubules. *ZFPD* 27(1), 93-96.

- G.Sun, G. Z. (2010). Preparation, crystallization, electrical conductivity and thermal stability of syndiotactic polystyrene/carbon nanotube composites. *Carbon* (48), 1434-1440.
- H .Li, W. Y. (2008). *IEEE transaction on electron devices Vol 55 No 6*.
- H.H.Gommans, J. A. (2000). *Journal of Applied Physics* 88, 2509-2514.
- H.Stahl, J. A. (2000). *Physics Review Letter*, 85, 5186.
- I.Dierking, G. P. (2005). *Journal of Applied Physics* 97, 044309.
- I.Heiskanen, A. ., (2011). *Patenttinro WO/2011/051882. FINLAND*.
- J. Du, L. Z. (2011). Comparison of electrical properties between multi walled carbon nanotube and graphene nanosheet / high density polyethelene composites with a segregated network structure. *Carbon* (49), 1094-1100.
- J. Nerg, M. V. (2012). Design of Direct Driven Permanent Magnet Synchronous Motors for an Electric Sports Car. *IEEE*.
- J. Zhu, H. G. (2012). Carbon Nanostructure derived Polyaniline Metacomposites: Electrical, Dielectric and Giant Magnetoresistive Properties. *American Chemical Society* (28), 10246-10255.
- J.Hone, M. M. (2002). Thermal Properties of carbon nanotubes and nanotube-based materials. *Applied Physics A- Matter Science Process* 74(3), 339-343.
- J.J.Vilatela, R. K. (2012). The hierarchical structure and properties of multifunctional carbon nanotube fiber composites. *Carbon* (50), 1227-1234.
- J.Jia, J. Z. (2011). A Comparison of the mechanical properties of fibers spun from different carbon nanotubes. *Carbon* (49), 1333-1339.
- J.N. Coleman, U. K. (2006). Small but strong: A reveiw of the mechanical properties of carbon nanotube-polymer composites. *Carbon* (44), 1624-1652.
- J.P.Lu. (1997). Elastic properties of single and multilayered nanotubes. *JOurnal of Physics and Chenistry Solid* 58 (11), 1649-1652.
- J.V. Silicone, D. L. (2013). *Fluidization and mixing of nanoparticle agglomerates assisted via magnetic impaction*. Springer Science+Media Dordrecht.
- J.W.Che, T. W. (2000). Thermal conductivity of carbon nanotubes. *Nanotechnology* 11(2), 65-69.

- J.W.G.Wildoer, L. (1998). Electronic structure of atomically resolved carbon nanotubes. *Nature*, Vol 391, 59-62.
- K.Liu, Y. S. (2010). Carbon Naotube yarns with high tensile strength made by a twisting and shrinking. *Nanotechnology* (21), 045708.
- K. Bubke, H. G. (1997). Optical anisotropy of dispersed carbon nanotubes induced by an electric field. *Applied Physics Letter* 71(14), 1906-8.
- K. L. Jiang, Q. Q. (2002). *Nature* 419, 801.
- K.Gong, F. Z. (2009). *Nitrogen-Doped Carbon Nanotube Arrays with High Electrocatalytic Activity for Oxygen Reduction*. Science Vol 323.
- K.H. Kim, M. M. (2011). Single Walled carbon Nanotube Aerogel based Elastic Conductors. *Advanced Material* (23), 2865-2869.
- K.Koziol. (2007). High performance carbon nano fiber. *Science* 318, 1892.
- K.R. Reddy, B. S. (2009). Conducting polymer functionalized multi-walled carbon nanotubes with noble metal nanoparticles: Synthesis, morphological charateristics and electrical properties. *Synthetic Metals* (159), 595-603.
- K.V.K. Boodhoo, S. R.-H. (2012). *Micromixing Charateristics in a small scale spinning disc reactor*. newcastle University, School of Chemical engineering and Advanced Materials.
- L.Aryasomayajula, K. W. (2013). Carbon nanotube Composite for Electronic Packaging Applications: A review. *Journal of nanotechnology*, article 296517.
- L. M. Ericson, H. F. (2004 ). Macroscopic, neat, single walled carbon nanotube fibers. *Science* (305), 1447-1450.
- L.Hu, D. H. (2010). Carbon Nanotube Thin Films: Fabrication, Properties and Applications. *Chemical reviews*, vol 110, no 10, 5793.
- M.Zhang, K. A. (2004 ). Multifunctional carbon nanotube yarns. *Science* (306), 1358.
- M. F. Islam, E. R. (2003 ). *Nano Letter* , 3, 269.
- M. Fujii, X. Z. (2005). Measuring the Thermal Conductivity of a Single Carbon Nanotube . *Physics Review Letter* (95).

- M.A.Osman, D. (2001). Temperature dependence of the thermal conductivity of single-wall carbon nanotubes. *Nanotechnology* 12(1), 21-24.
- M.A.Worsley, S. K. (2009). Mechanically robust and electrically conductive carbon nanotube foams. *Applied Physics Letter* (94).
- M.Arnold. (2008). *Nature nanotechnology*. Found in [http://www.nature.com/nnano/journal/v3/n7/fig\\_tab/nnano.2008.135\\_F1.html](http://www.nature.com/nnano/journal/v3/n7/fig_tab/nnano.2008.135_F1.html)
- M.B.Jakubinek, M. J. (2012). Thermal and electrical conductivity of array spun multiwalled carbon nanotube yarns. *Carbon* (50), 244-248.
- M.B.Jakubinek, M. W. (2010). Thermal and Electrical conductivity of tall, vertically aligned carbon nanotube arrays. *Carbon* (48), 3947-3952.
- M.D.Lynch, D. (2002). *Nano Letter* 2, 1197.
- M.Endo, T. Y. (2006). Large scale production of carbon nanotubes and their applications. *Pure Applied Chemistry* 78, 1703.
- M.F.Yu, O. M. (2000). Strength and breaking mechanism of multiwalled carbon nanotubes under tensile loads. *Science Vol 287 no 5453*, 637-640.
- .M.Shulaker, G. H. (2013). Carbon nanotube computer. *Nature, Vol 501* , 526-530.
- M.Monthieux, V. (2006). Who should be given the credit for the discovery of carbon nanotubes? *Carbon, vol 44, issue 9*, 1621-1623.
- M.S.Dresselhaus, G.D,P.C.E (1996) *Science of Fullerenes and Carbon Nanotubes: Their Properties and Application, Academic Press*
- M.S.P.Sarah, F. U. (2012). Conductivity Enhancement of Nanocomposited MEH PPV: I-MWNT Thin Film. *IEEE*.
- M.S.Strano, C. D. (2003). *Science,301*, 1519.
- M.Yu, O. M. (2000). Strength and breaking mechanism of multiwalled carbon nanotubes under tensile load. *Science* 287, 637-640.
- msu.edu*. (ei pvm). Found in <http://www.pa.msu.edu/cmp/csc/ntproperties/equilibriumstructure.html>
- N Grossiord, J. L. (2008). High Conductivity Polymer nanocomposites Obtained by Tailoring the Characteristics of Carbon Nanotube Fillers. *Advanced Functional Materials* (18), 3226-3234.

- N.Behabtu, C. C. (2013). Strong, Light, Multifunctional Fibers of Carbon Nanotubes with Ultrahigh Conductivity. *Science* 339,182.
- N.Grossiord, P. J. (2008). On the influence of the processing conditions on the performance of electrically conductive carbon nanotube/polymer nanocomposites. *Polymer* (49), 2866-2872.
- N.Pugno, F. (2009). Scaling Properties of nanotube based Macroscopic Cables through multiscale numerical simulation. *IEEE Nanotechnology magazine*.
- O .Matarredona, H. Z. (2003). *Journal of Physical Chemistry B*, 107, 13357.
- O.K. Park, T. .. (2009). Effects of surface modification on the dispersion and electrical conductivity of carbon nanotube/polyaniline composite. *Scripta Materiala* 60, 551-554.
- P. Guichardon, L. F. (2000). *Chem Eng Sci* 55(19), 4233.
- P.N. Nirmalraj, P. L. (2009). Electrical Connectivity in single Walled carbon Nanotube networks. *Nano Letters*, Vol 9, No 11, 3890-3895.
- PL McEuen, S. F. (2002). Single Walled Carbon Nanotube Electronics. *Nanotechnology Vol 1 No 1*.
- Pyrhonen, J. (2008). *Design of rotating electrical machine*. Willey and Sons.
- Q. Cao, J. R. (2009). *Advanced Materials*, 21, 29-53.
- Q. Cheng, J. B. (2009). High Mechanical Performance Composite Conductor: Multi Walled Carbon Nanotube Sheet / Bismaleimide Nanocomposites. *Advanced Functional Materials* (19), 3219-3225.
- Q. Li, Y. L. (2007). Structure Dependent Electrical Properties of Carbon Nanotube Fibers. *Advanced Material*.
- Q. Zhang, J. Q. (2011). Carbon Nanotubes mass production: Principles and Processes. *ChemSusChem* 4, 864.
- Q.Chen. (2007). *Patenttinro 2007/0036978A1, Feb15 2007*. US.
- Q.P. Feng, J. Y. (2010). Synthesis of carbon nanotube/epoxy composite films with a high nanotube loading by a mixed curing agent assisted layer by layer method and their electrical conductivity. *Carbon* (48), 2057-2062.

- R.Basu, C. L. (2011). Carbon nanotube induced macroscopic helical twist in anachiral nematic liquid crystal. *Journal of Applied Physics* 109, 083518.
- R.Graupner, J. A. (2003 ). Doping of single walled carbon nanotube bundles by Bronsted acids. *Physical Chemistry Chemical Physics* (5), 5472-5476.
- R.H. Baughman, A. W. (2007). Carbon Nanotubes- The route toward applications. *Science 's Compass*.
- R.H.Baughman, C. C. (1999). Carbon nanotube actuators. *Science*, 289, 1340-4.
- R.Maldzius, P. J. (2010). Temperature dependance of electrical and dielectrical properties of paper for electrophotography. *Journal of Applied Physics* 107, 114904.
- S. Pei, J. Z. (2010). Direct reduction of graphene oxide films into highly conductive and flexible graphene films by hydrohalic acids. *Carbon* (48), 4466-4474.
- S.Ghosh, S. M. (2010). Advance sorting of single walled carbon nanotubes by non linear density gradient ultracentrifugation. *Nature Nanotechnology* 5, 443-450.
- S.H. Lee, E. C. (2007). Rheological and electrical properties of polypropylene composites containing multiwalled carbon nanotubes and compatibilizers. *Carbon* (45), 2810-2822.
- S.Hong, S. M. (2007 ). Nanotube electronics: a flexible approach to mobility. *Nature Nanotechnology* (2), 207-208.
- S.Jayronia, A. S. (2013). Carbon nanotube- a burgeoning field in nanotechnology. *World journal of pharmaceutical research* 3(1), 295-310.
- S.K.Manna, S. S. (2005). Single Walled Carbon nanotube induces oxidative stress and activates nuclear transcription factor kB in Human keratinocytes. *Nano Letters* 5(9), 1676-1684.
- T. Maitra, S. S. (2012). Improved graphitization and electrical conductivity of suspended carbon nanofibers derived from carbon nanotube/polyacrylonitrile composites by directed electrospinning. *Carbon* (50), 1753-1761.
- T.C. Theodosiou, D. S. (2010). Numerical Investigation of mechanisms affecting the piezoresistive properties of CNT doped polymers using multi scale models. *Composites Science and Technology*, 70(9), 1312-20.
- T.V.Sreekumar, T. B. (2004). *Advance Material* 16, 58-61.

- U. Khan, I. C. (2010). The preparation of hybrid films of carbon nanotubes and nano-graphite/graphene with excellent mechanical and electrical properties. *Carbon* (48), 2825-2830.
- U.D .Wegilikowska, V. .. (2005). Effect of SOCl<sub>2</sub> Treatment on Electrical and Mechanical Properties of Single Wall Carbon Nanotube. *J A CS Articles*.
- W. Zhou, J. V. (2004). *Journal of Applied Physics* 95, 649-655.
- V.A.Davis, M. P. (2004). *Nanoengineering of structural, functional and smart material, ch 11*. CRC Press.
- W.K.Yeoh, J. J. (2007). Effect of Carbon Substitution on the superconducting properties of MgB<sub>2</sub> Doped with multiwalled Carbon nanotubes and Nano Carbon. *IEEE transactions on applied superconductivity*. IEEE.
- V.P.Veedu. (2006). Multifunctional composites using reinforced laminated with carbon nanotube forests. *Nature Material*5, 457.
- W.Soliman, T. .. (2013 ). A novel Electro Thermal Model for Carbon Nanotube Interconnects. *Journal of American Science*, 9(4), 511-518.
- W.Y.Yong, W. D. (2012). Effect of Nitrogen doping concentration nanotubes on cathodic performance for proton exchange membrane fuel cell. IEEE.
- Williams, M. (2014). *Rice's carbon nanotube fibers outperform copper*. Found in Found in <http://news.rice.edu/2014/02/13/rices-carbon-nanotube-fibers-outperform-copper-2/>
- X. Liu, J. S. (2004). Electric field oriented carbon nanotubes in different dielectric solvents. *Current Applied Physics*, 4, 125-8.
- X.B. Zhang, K. J. (2006 ). Spinning and processing continuous yarns from 4 inch wafer scale super alligned carbon nanotube arrays. *Advanced Materials* (18), 1505-1510.
- X.H. Li, J. Z. (2003). *Carbon* 41, 98-601.
- Y. Li, I. K. (2004). Direct spinning of carbon nanotube fibers from chemical vapor deposition synthesis. *Science* ,304, 276-278.
- Y. Zhao, J. R. (2011). Iodine doped carbon nanotube cables exceeding specific conductivity of metals. *Nature, Science Report*.

- Y.J. Kim, T. S. (2005). Electrical conductivity of chemically modified multiwalled carbon nanotube/epoxy composite. *Carbon* ( 43), 23-30.
- Y.Li, H. .. (2009). Toward a Stretchable, Elastic, and Electrically Conductive Nanocomposite: Morphology and properties of Poly[styrene-b-(ethylene-co-butylene)-b-styrene]/Multiwalled Carbon Nanotube Composites Fabricated by High-Shear Processing. *Macromolecules* (42), 2587-2593.
- Y.Liu, L. D. (2012). Macroscopic shaping of carbon nanotube with high surface area and full accessibility. *Materials Letters* 79, 128-131.
- Y.T. Park, A. H. (2010). High Electrical Conductivity and Transparency in Deoxycholate Stabilized carbon Nanotube Thin Films. *Journal of Physics Chemistry* (114), 6325-6333.
- Z. Spitalsky, D. T. (2010). Carbon nanotube-polymer composites: Chemistry, processing, mechanical and electrical properties. *Progress in Polymer Science* (35), 357-401.
- Z.K.Tang, L. N. (2001). Superconductivity in 4 Angstrom single walled carbon nanotubes. *Science* 292(5526), 2462-2465.
- Z.Yao, C. C. (2000). High Field Electrical Transport in Single Wall Carbon Nanotube. *Physical Review Letters*, Vol 84, No 13, 2941-5.